This is to certify that the
dissertation entitled

PLANT-ENHANCED REMEDIATION OF NAPHTHALENE

presented by

CHRIS M. SAFFRON

has been accepted towards fulfillment
of the requirements for the

Doctoral degree in Chemical Engineering and Materials Science

Major Professor's Signature

AUGUST 25, 2005

Date

PLANT-ENHANCED REMEDIATION OF NAPHTHALENE

By

Chris M. Saffron

A DISSERTATION

Submitted to
Michigan State University
in partial fulfillment of the requirements
for the degree of

DOCTORATE OF PHILOSOPHY

Department of Chemical Engineering and Materials Science

2005

ABSTRACT

PLANT-ENHANCED REMEDIATION OF NAPHTHALENE

By

Chris M. Saffron

This study explored the effects of slow desorption on the rate of removal of naphthalene in planted systems. The magnitude by which desorption limits the removal of PAHs was assessed in different soils. The contaminant exhibited nonequilibrium desorption in all of the soils studied. The desorption data were described using several desorption models. The desorption models were also used to quantify the rate of mass transfer from the soil solute to the soil solution. The mathematical models were ranked using a construct called the Akaike Information Criterion, which takes into account accuracy and parameter variability. The effect that plants have on the rate of naphthalene removal in soils was also assessed. The collected data was interpreted using a descriptive model. Volatilization by gaseous diffusion, sorption to roots, transpirational uptake, fast mass transfer from the soil solid, and slow mass transfer from the soil solid were included in the model.

The lessons learned during the development of this model were used in positing a decision-making methodology. This methodology contains a procedural approach for quantifying the rate of mass transfer, and whether plants are able to overcome these transfer limitations. A dimensional analysis was used to determine the efficacy of planted systems, which leads to improved decision making regarding phytoremediation.

This work is dedicated to my wife, Danida.

ACKNOWLEDGMENTS

I would like to acknowledge the effort and patience that my wife, family, and friends have given me throughout this journey. My wife, Danida, has exhibited degrees of patience, support, and love that I thought not possible. I thank my family for their continuing encouragement and unwavering support. I thank my Mom, and my Grandma and Grandpa Swanson for the work ethic that they've instilled in me since childhood. I would not have done this without them. I thank God for the joy he has brought my wife and I, especially since the birth of our daughter Annaka. I am grateful to the many friends that I've made while in graduate school. I extend special thanks to Dr. Jeong-Hun Park, for his insight and thoughtfulness. I thank Dr. Mazen Haydar for many stimulating conversations. I thank Dr. Irfan Aslam for discussions about desorption in column studies, and a unique way of making a lay-up. I thank Shawn McElmurry for discussions concerning the environment and recreational activities. I thank Dr. Robert Dombrowski, Dr. David Knop, and Dr. Prashant Srivastava for the many homework sessions and discussions regarding chemical engineering. Thanks to Dr. Clayton Rugh and the Phytolab crew for the lessons in sterile technique and the trips to Oodles of Noodles. Finally, I would like to thank Professors Bruce Dale and Thomas Voice. Your advisement has kept me on target through a very challenging portion of my life. And now, the real challenge begins.

TABLE OF CONTENTS

LIST OF TABLES

LIST OF FIGURES

Chapter 1. Introduction and objective

Introduction

Currently, the world oil consumption is estimated at 75 MM barrels of oil per day[1]. This corresponds to filling a cube with sides that are roughly 1 mile wide every year. This amount of production/consumption provides an ample driving force for contamination of soils, waterways and air with organic contaminants. The remediation of organic contaminants by plants has become a viable alternative to more traditional schemes. Currently, phytoremediation is being used by academia, industry, government and the military to remediate sites contaminated with polyaromatic hydrocarbons (PAHs), polychlorinated biphenyls (PCBs), trichloroethylene (TCE), perchloroethylene (PCE), trinitrotoluene (TNT), and many others. When compared to competing technologies, such as excavation and incineration, pump and treat, etc., phytoremediation has several inherent advantages. In addition to being an effective technology for clean-up, advantages include: a relatively low cost, a general social acceptance, an aesthetically pleasing appearance over competing technologies and the support of a diverse and burgeoning population of trained professionals. Like microbial bioremediation, phytoremediation is an *in situ* technology that will not disturb the soil matrix. Phytoremediation takes advantage of a plant's innate ability to transpire water, which concentrates dilute contaminants. The bacterial population in rhizosphere soils is also ten to 1000 times greater than in unplanted bulk soil[2]. As much as 30 percent of a plant's photosynthate is exuded in the roots[2], and many of these exudates resemble organic

contaminants[2] (a feature of plants that may induce degradative enzymes or prompt cometabolism). Plants are known to improve soil aeration, soil aggregation, reduce erosion, and fix atmospheric carbon dioxide. Though planting, monitoring, amending with nutrients, harvesting and disposal are costs associated with phytoremediation—the energy required for growth is provided by sunlight and a plant's ability to acquire dilute nutrients by transpiration provides a concentrating effect in the root zone. Cunningham and Berti have stated[3]:

> "A green plant is a 'solar-driven, pumping, and filtering system that has measurable loading, degradative and fouling capacity'. Roots are 'exploratory, liquid-phase extractors that can find, alter, and/or translocate elements and compounds against large chemical gradients'".

In truth, the complexities inherent in phytoremediation systems include many mechanisms not included in the above description. Thus, given the obvious need for remediation and clean-up, and including the advantages that phytoremediation has over other technologies, further development in this area is warranted. The proper selection of remediation technologies that are demonstrated effective, that are low-cost, and that can add aesthetic value is of the utmost importance.

In 1999, the estimate for the total U.S. phytoremediation market exceeded 30 MM U.S. dollars[4]. This number will grow, as it is estimated that 1.7 trillion U.S. dollars will be spent on clean-up in the U.S. over the next thirty years[5]. Cost

estimates for design and implementation ranged between 60,000 to 100,000 U.S. dollars per acre in 1999. This is roughly one-fourth the cost of excavation followed by landfilling[6]. Further evidence supporting the efficacy of phytoremediation of organic pollutants in soils will expand the market for this technology.

Objectives

This study was designed to explore the effects of slow desorption on the rate of remediation in planted systems. Four objectives were considered in this investigation. The chapters of this dissertation are organized around each of these objectives.

The first objective is to assess the magnitude that desorption limitations may impose on planted systems. All of the studied soil and contaminant combinations exhibited nonequilibrium desorption phenomena, meaning that desorption from the soil matrix may limit the rate of remediation. Several mathematical models were fit to each set of desorption data to describe the rate of desorption. The mathematical models were ranked based on accuracy and parameter variability using a construct called the Akaike Information Criterion. The knowledge that was gained concerning the desorption limitations was used to design the experiments needed to satisfy the second objective of this study.

The second objective was to determine the effect plants have on contaminated soils that are limited by slow desorption. Completion of this objective would provide evidence that phytoremediation is or is not limited by slow desorption from the soil matrix.

The third objective was to formulate a descriptive model that fits the rate data collected during the completion of the second objective. The model was developed as a descriptive tool, i.e. a tool used to interpret the collected data. Several types of mass transport were considered in the model development, including: volatilization by gaseous diffusion, root uptake by sorption to lipophilic tissues, transpirational uptake, fast mass transfer from the soil solid, and slow mass transfer from the soil solid. Mechanisms that did not add to organic chemical mass transfer under the study conditions of the second objective were not included in the model, e.g. the advection and dispersion due to contaminant leaching. The lessons learned during the development of this descriptive tool were used in positing a decision-making methodology, which forms the basis of the fourth objective.

The fourth objective involves the use of a mathematical model, developed using the lessons learned upon completion of the first three objectives, for developing a decision-making methodology. This methodology contains a procedural approach to determining whether organic mass transfer from the soil is limiting in batch conditions, and whether plants are able to circumvent these transfer limitations. The analysis will be conducted using the classical approach of dimensional analysis. After the interpretation of the collected data using a constructed mathematical model, plotting the dimensionless groups results in a division between a mass transfer limited regime and a reaction rate limited regime. The decision regarding the use of phytoremediation can be made by interpreting the plots of dimensionless groups.

References

1. Abraham, S., *Remarks by Energy Secretary Spencer Abraham Public Energy Forum Lunch Conference of G8 Energy Ministers*. May 2, 2002: Detroit, Michigan.

2. Curl, E.A. and B. Truelove, *The Rhizosphere*. 1986: Springer-Verlag Berlin Heidelberg.

3. Cunningham, S.D. and W.R. Berti, *Remediation of contaminated soils with green plants: an overview.* In Vitro Cellular and Developmental Biology, 1993. **29**: p. 207-212.

4. Glass, D., *U.S. and International Markets for Phytoremediation, 1999-2000.*

5. Timian, S.J. and D.M. Connely, *The Regulation and Development of Bioremediation.* 1996.

6. Marmiroli, N. and S.C. McCutcheon, *Making Phytoremediation a Successful Technology*, in *Phytoremediaiton: Transformation and Control of Contaminants*, S.C. McCutcheon and J.L. Schnoor, Editors. 2003, John Wiley and Sons, Inc.

Chapter 2. Literature Review

Introduction

The effort presented in this chapter reviews many of the published mechanisms responsible for controlling the rate and extent of phytoremediation. The numerous processes involved in phytoremediation are investigated to assess which may limit the application of this technology. In actuality, phytoremediation encompasses several technologies, and a short description of the various technologies is presented in this chapter and summarized in Table 2-1. Many of the processes involved in the phytoremediation technologies have been previously assembled into mathematical models by other authors—several of these models are reviewed in this chapter. The modeling investigations presented in the literature assume that equilibrium exists between the soil matrix and the soil solution, while the investigation presented in Chapters 3 and 4 of this dissertation explores the kinetic limitations of contaminant desorption. Furthermore, an obvious link between the effort *in vitro* and the effort *in situ*, regarding the use of mathematical models describing phytoremediation, does not appear to exist. Chapter 5 of this dissertation attempts to bridge the gap between a descriptive model and a decision-making tool that would benefit the application of phytoremediation by the site engineer

Phytoremediation is defined as the use of green plants to remove pollutants from the environment or to render them harmless[1]. This is a burgeoning technology that can be used for a diverse array of contaminant-soil combinations. The number of applications for phytoremediation has increased as the collective understanding, concerning the root-soil-contaminant interaction, has improved. Plants have been

effectively demonstrated to remediate soils contaminated with several classes of contaminants, including: organic contaminants[2-11], heavy metal contaminants[12-17], and radionuclide contaminants[18, 19]. Several phytoremediation technologies exist for removing these contaminants, including those listed in Table 1. This review contains a brief summary of these technologies, some of the mechanisms controlling these technologies, and the models that are capable of describing the controlling mechanisms. The last section of this review presents the scope of the research that is contained in the following chapters.

Phytoremediation technologies

Several studies have validated the use of phytodegradation. Poplar trees were found capable of transforming trichloroethylene (TCE) to trichloroethanol, trichloroacetic acid, and dichloroacetic acid[20]. The ability of plant cell culture and plant cell extracts were found capable of transforming glycerol trinitrate (nitroglycerin) to glycerol dinitrate and later, glycerol mononitrate[21]. Nitroreductase and laccase enzymes, released by plants, were shown to degrade 2,4,6-trinitrotoluene (TNT)[2]. Symbiotic bacteria were found in poplar that are capable of degrading TNT, high melting explosive (HMX), and royal demolition explosive (RDX)[22]. Enhanced microbial degradation was likely responsible for the removal of petroleum hydrocarbons from the rhizosphere of sorghum[23]. In general, the phytodegradation of contaminants can occur within the plant tissue by transformation (either by enzymes or endophytes), or *ex planta* by plant-released enzymes or the microbial consortia (known as rhizodegradation). Less well demonstrated is the occurrence of phytostimulation, though a few studies have provided interesting results. The mineralization of atrazine was promoted by the addition of root

exudates into silica sand and silt loam filled microcosms[24]. The stimulatory effect of root exudates is a possible explanation for the enhanced microbial degradation of pentachlorophenol in the rhizosphere of Hycrest crested wheat grass[25]. The removal of polychlorinated biphenyls (PCBs) in the rhizosphere of red mulberry was attributed to the stimulatory action of phenolics on the rhizosphere consortia[26]. Contrarily, the addition of root extracts was shown to decrease the expression of *nahG* using *Pseudomonas fluorescens* HK44 (this contains a *nah-lux* fusion), though the total amount of expression was increased due to increased cell growth upon extract addition[27]. The use of phytoremediation to stimulate the microbial consortia to degrade contaminants is an area of ongoing research. Other phytoremediation technologies are being practiced in the field and investigated in academia. The use of phytoextraction[28], both chelate-assisted and unassisted is perhaps the most well documented mode of phytoremediation. It has been mathematically determined that the evaporative flux from a stand of trees used in phytocontainment of a TCE plume, must be much greater than the flux of the plume itself[29]. Phytovolatilization of methyl *tert*-butyl ether (MTBE) was found to occur through the stem and leaves of poplar cuttings[30]. Phytostabilization may be especially useful for controlling tailings from strip and open uranium mines[31]. Other phytoremediation technologies exist in addition to those mentioned in this review, though phytodegradation and phytostimulation are the most relevant phytoremediation technologies for the effort presented in this dissertation.

Processes involved in phytoremediation

The effective use of phytoremediation depends upon an understanding of the mechanisms that control the rate of removal in the rhizosphere. The word "rhizosphere"

is loosely defined as the soil zone influenced by the roots[32]. This zone contains the soil solid (soil matrix), the soil solution, soil gas, the plant roots, and all rhizosphere microbes. Many chemical, physical, and biological processes occur in the rhizosphere[32-34]—and often these processes interact in a complex manner. A simplified depiction of the nature of these interactions is as shown in Figure 1. As with bulk soil, the rhizosphere soil can be characterized chemically, in terms of its soil organic matter (SOM) content, and physically, in terms of its porosity and texture. Biologically, a multitude of microorganisms, both in numbers and in types, exist in the rhizosphere[32, 34]. These organisms can interact with plants by secreting plant growth promoting hormones[35]. Plants can influence the quantity and types of organisms, in the microbial community, through root exudation[24, 36, 37] (a passive process) or root secretion (an active process). Plants alter the chemistry of the soil solution through the process of transpiration. The transpirational movement of water towards the root serves to concentrate dilute nutrients in the rhizosphere. Through a combination of physical, chemical, and biological processes that occur in the rhizosphere, the manner and degree of soil aggregation can be affected[38]. The degree of aggregation can alter the level of soil aeration and the level of moisture infiltration[38]. The growth of roots into the soil matrix can also increase soil aeration and moisture infiltration by opening channels that locally increases the soil conductivity. The complex interaction between biological, chemical and physical processes is further demonstrated by lignin deposition. Lignin, a component of plant cell walls, is an important component during the formation of soil organic matter (SOM)[39]. Therefore the physicochemical properties of the soil matrix are affected by root growth and necrosis. Essentially, a number of processes are

simultaneously occurring in the rhizosphere, which creates a highly complex, versatile, and dynamic zone with the proposed potential for remediating hazardous compounds.

The transport and transformation of an organic contaminant in the rhizosphere is of interest to scientists and engineers who want to explain the observed rates of contaminant loss and apply the technology to contaminated sites. The rate of contaminant loss can be controlled by: 1) mass transfer limited desorption of the contaminant from the soil matrix, 2) the microbial biodegradation rate in the soil solution, 3) the rate of sorption to the plant root, 4) the rate of transpirational uptake, 5) the rate of volatilization and 6) the rate of leaching. Other mechanisms that may allow planted systems an advantage over unplanted systems include the release of oxidative enzymes from the root, the exudation of molecules that compete for sorption sites with the contaminant, or degradation by mycorhizal fungi. The aforementioned six mechanisms are under consideration in this work, due to the preponderance of evidence that suggests these mechanisms are universally important when considering the application of phytoremediation.

The mechanism that is most likely to limit the rate and extent of a contaminant's remediation by plants is mass transfer limited desorption. The likely first step in a contaminant's removal is desorption. The rate of phytoremediation will equal the rate of desorption, when no mechanism exists for enhancing the desorption rate. Conceptually, the rate of desorption is limited by the mass transfer of the compound from the soil matrix to the soil solution. The desorption rate depends on the path length, path tortuosity, physicochemical properties of the matrix, and the physicochemical properties of the contaminant[40, 41]. Furthermore, the desorption rate can change as organic

contaminant desorbs from the soil[42-46]. Desorption rate data has suggested that more than one type of phenomena is responsible for controlling the rate and extent of HOC desorption[47-51]. The desorption profile can be described by assigning the collected desorption data into one, two or three conceptual regimes. Historically, a one-regime model that assumes sorption-desorption reversibility, was used to describe the desorption process in batch and flow-through systems. Conceptually, desorption was thought to be an equilibrium process which occurred instantaneously upon addition of aqueous solution. This equilibrium process is parameterized by the soil-water partition coefficient, which is a thermodynamic construct that is measured by plotting a sorption isotherm. The use of the soil-water partition coefficient assumes a negligible sorption-desorption hysteresis, an assumption that often over-predicts the extent and rate of desorption. In reality, desorption usually occurs at a slower rate than sorption. Thus the one-regime model of contaminant desorption was found to be inadequate in predicting the extent and rate of contaminant desorption for many systems. The advent of the two-regime model was spurred by consideration of mass transfer limitations that may be inherent in soil matrices. These models are constructed to include characteristics attributable to equilibrium phenomena and characteristics attributable to kinetic phenomena. These models were formulated to describe desorption data that are exemplified by fast desorption followed by slow desorption. Many explanations exist for the kinetic phenomena that limit the rate at which contaminant desorbs from the soil. Two classes of kinetic phenomena are distinguished in the literature. These are the kinetic phenomena attributable to: 1) the chemical characteristics of the contaminant and soil matrix, and 2) the physical characteristics of the contaminant and soil matrix. The chemical two-regime models

assume that a chemical interaction between the contaminant and the solid matrix acts to retain the contaminant beyond what is predicted by chemical equilibrium. The physical two-regime models assume that a physical constraint retards the passage of contaminant through the soil matrix. The use of a Fickian diffusive flux is normally used to describe the transport of contaminant through a soil micropore, through the soil organic matter, or through immobile water regimes. The main advantage of the two regime models is the ability to describe desorption data that exhibits two distinct classes of behavior. However, when the extent of contaminant desorption is less than one-hundred percent after sequential water extraction (i.e. batch desorption) studies or flow-through (i.e. column desorption) studies, the two regime models do not accurately describe the collected data. In this circumstance, the formulation of three regime models was needed to accurately describe the data[52]. These models were built using the two-regime models, with the addition of a third regime that accounted for material that sorbed but did not desorb. Irreversible chemical binding and pore clogging by mineral precipitates are two explanations for desorption resistance. Regardless of the explanation, this regime appears to retain organic contaminant for extensively long durations. The ability to describe three distinct types of behavior is the advantage of using a three-regime model. Other models for desorption exist in the literature, and are often of mixed physical and chemical nature. For example, the multi-process nonequilibrium model divides the kinetic behavior into a mobile and an immobile regime[53], as is the case in most physical models. This model accounts for chemical nonequilibrium in each of the physical regimes. The gamma distribution model[42] uses the gamma distribution function from statistics to arbitrarily divide the soil into fractions that transfer mass at

different rates. This model, and the subsequent hybrid gamma/two-site model[47], provide an empirical description of the desorption phenomena. To date, no general consensus has been reached regarding the use of desorption models to describe desorption data. The importance of applying state of the art desorption models lies in the accuracy needed to describe phytoremediation. Models of contaminant desorption, and the explanations that accompany these models, must be considered when formulating descriptive models for phytoremediation.

Microbial biodegradation of hydrophobic organic contaminants may also be a limiting process in the rhizosphere. Briefly, the ability of the consortia to degrade a compound at an appreciable rate depends upon the number of degrading microbes, their *in vivo* degradative capacity, and the bioavailability of the compound of interest. The number of degrading organisms is likely to be increased in rhizosphere soils, as the plant roots are known to exude and secrete molecules that may cause enzymatic induction or prompt cometabolism[54]. For example, the exudation of phenolic materials is thought to promote the bacteria that are capable of degrading PCBs[55]. Even though recent evidence has suggested that the *in vivo* degradative capacity of the organisms is debilitated[56], increased degradation remains the net effect in the rhizosphere[56]. A net increase in rhizosphere soil over bulk soil is due to the comparative number of organisms in the rhizosphere. The rhizosphere can support over two orders of magnitude more microbes than unplanted soil. However, even with greater numbers, the rhizosphere population may still be limited by constraints on bioavailability. Thus, the bioavailability of hydrophobic organic contaminants is of great interest, as low bioavailability will limit the rate and extent of degradation. Soil-contaminant

combinations, that exhibit slow desorption, are candidates for bioavailability limitations. If the microbe, plant, or microbe-plant combination are not able to accelerate the desorption rate, the rate of degradation will not exceed the rate of desorption.

The plant roots provide a sink for HOCs, as a portion of the root tissue is composed of long-chain fatty acids and alcohols called suberin[57]. This waxy tissue is named the Casparian strip, and it is chiefly responsible for sorbing material that enters via the transpiration stream. The early effort into quantifying the potential for root sorption was performed using pesticides[58]. More recent studies have been performed on poplar sprigs placed in hydroponic media that is spiked with contaminants such as TCE[59]. The soil solution is assumed to be the sole contaminant source (i.e. direct transfer from the soil solid or soil gas is neglected). The amount of material present in the root tissue versus the soil solution is assumed to follow an equilibrium-type mechanism. The resulting equilibrium constant has been named the root concentration factor (RCF). The RCF is commonly estimated as an empirical function of the octanol-water partition coefficient. The total amount of contaminant sorbed to the root tissues is a function of the aqueous concentration of the contaminant and the total mass of the root tissue. This sorbed mass is likely small, as the root mass is relatively small compared to the mass of rhizosphere soil. Furthermore, rate-limited desorption from the soil matrix may limit the aqueous concentration, and thus the contaminant mass sorbed to the root.

Transpirational flow provides a significant source of dissolved nutrients and water to the plant, which are needed for plant health. The transpiration stream will also carry dissolved contaminant, carrying it to the stem and leaves. The development of a method for quantifying the transpirational uptake parallels the quantification of root sorption, as

outlined in the pesticide literature[58]. Like the computation of the RCF, the transpiration-stream concentration factor (TSCF) is computed using an equilibrium-type relationship. This relationship can be empirically related to the octanol-water partition coefficient. Therefore, the amount of contaminant in the transpiration stream is a function of the contaminant concentration in the soil solution. The mass of contaminant that is removed from the soil solution is a positive function of the transpiration stream flow rate and the contaminant concentration in the soil solution. The mass of contaminant that enters the transpiration stream may be limited by the rate of desorption from the soil matrix to the soil solution.

Volatilization from the soil occurs when a volatile chemical (i.e. a chemical with a high vapor pressure) enters the soil gas from either the soil solution or the soil solid. Assuming that the soil moisture content is at an appreciable level, the amount volatilization from the soil solid is usually neglected. For the case of dilute contaminant concentrations in the soil solution, the concentration of a volatile contaminant in the gas phase can be approximated using Henry's law[40, 41]. The Henry's law coefficient is an equilibrium-type expression that relates the gas phase concentration to the soil solution concentration. These values are extensively tabulated. In effect, the concentration in the soil gas is limited by the soil solution concentration, which may be limited by desorption from the soil matrix. Furthermore, if the soil harbors material that is not in equilibrium with the soil gas, e.g. material that resides in domains associated with microporous water, then this dissolved material is not to be included in the equilibrium expression. The equilibrium concentration of the volatile contaminant provides a driving force for flux out of the soil and into the above-ground atmosphere. The movement of contaminant in the

soil gas is assumed to occur primarily by Fickian diffusion. The Millington-Quirk correction is normally applied to the molecular diffusivity to adjust for the soil tortuosity[60]. The gaseous diffusion rate, is dependent upon the soil gas content, i.e. the volume of the air-filled voids. Planted systems can increase the volatilization rate by transpiring water, which increases the air-filled void volume and promotes a greater mass of material to equilibrate with the soil gas. Increasing the air-filled void volume also increases the soil gas diffusivity, as the flow path becomes less tortuous. Consideration of volatile and semi-volatile transport in the soil gas is important as much of this material will exit the system in the vapor phase.

Contaminant leaching, particularly with low to moderately hydrophobic materials, is a mechanism that occurs in planted and unplanted soils alike. Leaching is caused by the infiltration of water[61]—a process that removes contaminants from the rhizosphere. The magnitude of leaching depends upon the amount of water that is infiltrating the rhizosphere soil and the amount of contaminant dissolved in the mobile soil solution. As the plant roots increase the soil porosity[33], the potential for contaminant leaching that can occur during water infiltration is also increased. In this case, slow desorption from the soil matrix is an advantage as contaminant leaching is minimized. Nevertheless, the impact of leaching must be assessed when applying phytoremediation as a clean-up technology.

Review of modeling efforts

Several conceptual models have been formulated to describe the action of plant roots in the rhizosphere. Ultimately, these model formulations are based partly on

chemical equilibrium between compartments, certain kinetic interactions between compartments, and mass flow between compartments. Figure 2-1 contains a simplified model of the interactions between processes that are occurring in the rhizosphere. Often, the concept of rate limited desorption has not been considered in the model formulations. The following paragraphs contain a brief review of the models presented in the literature for describing the effect of phytoremediation on organic contaminants.

An early model of phytoremediation proposed that the degradation of contaminants in the rhizosphere is governed by a series of mass balances[62]. Balances were included for the contaminant, the microbial biomass, the root exudates, and dissolved oxygen. This resulted in the formulation of four, coupled partial differential equations in time and in two spatial dimensions. Equilibrium-type formulations were used to describe desorption from the soil, sorption to the roots, and partitioning into the plant's transpiration stream. Microbial growth was assumed to follow a Monod kinetic model. Diffusion and advection in the soil solution occurred in two dimensions, as did diffusion in the soil gas. The Henry's law coefficient was used to describe the relative amounts of contaminant in soil air and soil solution. A similar Henry's law model was used for soil oxygen. Though this model is relatively comprehensive—noticeably missing is a mechanism that is responsible for rate-limited desorption from the soil matrix.

A more recent phytoremediation model divides the planted system into several compartments[63]. The compartments include: saturated and vadose zone soil; saturated and vadose zone water; nonaqueous-phase liquid (NAPL); bacterial metabolism in the saturated zone, the vadose zone, and the root zone; plant metabolism of contaminants in

the root water, the stem water, and the leaf water; equilibrium-type sorption-desorption between each solid phase and its associated liquid phase (e.g. the use of the soil-water partition coefficient for determining the relative concentrations of contaminant in the vadose zone water and the vadose zone soil); Henry's partitioning between each liquid phase and its associated gas phase (e.g. the root water and the root gas phase); and gas diffusivity to account for the volatilization flux. Though this model is relatively comprehensive, it does not include a mechanism for rate-limited desorption from the soil matrix.

An investigation regarding the enhanced bioremediation of non-volatile hydrocarbons by plants[64] considered many of the same mechanisms previously described. An additional kinetic mechanism for contaminant degradation in a microbial biofilm was included in this model formulation. These biofilms are claimed to surround the roots and the simulation results suggested that enhanced degradation is due to biofilm metabolism. The fact that mass transfer from the soil solid to the soil solution could limit the rate of degradation in the biofilm was not addressed.

Contrary to many of the other models in the literature, Burken and Schnoor developed a model that does include a mechanism accounting for slow mass transfer from the soil[24]. This model was developed for assessing the rate processes that occur in the planted bioreactors. These bioreactors contain soil that is contaminated with atrazine. This model, relatively simple in formulation, contains compartments for slow and fast atrazine desorption into the aqueous phase, microbial mineralization from a bioavailable fraction of atrazine in soil, mineralization from the aqueous phase, and plant uptake. Slow desorption was found to limit the mobility of contaminant in soils with an

appreciable organic matter content. However, no evidence of enhanced desorption from desorption-resistant (i.e. non-desorbing regimes of soil) domains was explored.

The models developed for phytoremediation are relatively complex. It remains to be seen whether much of this complexity is warranted for describing the data. The development of a conceptual model, including mechanisms for rate limited desorption, may be necessary to accurately describe the effect plants have on organic contaminants. The experimental approach, presented in the following chapters of this dissertation, was designed to assess the magnitude that desorption-resistance has on the overall rate of phytoremediation. Contrary to the aforementioned models, and because of the inherent complexity of the model formulation, a dimensional analysis will be developed to simplify the interpretation of the resultant data. This dimensional analysis will be used to develop a decision-making framework that can be used to aid the site engineer in applying a phytoremediation technology.

Research scope

The scope of the following chapters is centered on the phytoremediation of organic compounds, specifically the PAHs (polyaromatic hydrocarbons). As seen in Table 2-1, the plant-assisted remediation of PAHs is thought to be accomplished by phytostimulation. By releasing compounds with a PAH-like chemical nature, the members of the microbial consortia that are capable of degrading PAHs are stimulated. These microbes then degrade PAH contaminants by transformation or cometabolism. The caveat exists in the presumption that the PAHs are bioavailable in the rhizosphere, which may not be true. An analysis is needed to determine the rate of mass transfer that

may limit PAH removal in the rhizosphere. Slow mass transfer of PAHs from the soil matrix may limit the bioavailability of PAHs. Slow mass transfer does not invalidate the efficacy of phytoremediation as a clean-up technology, though it does prompt the judicious selection of plant species for hastening desorption. A plant's ability to enhance the desorption of hydrophobic organic contaminants (HOCs), like the PAHs, would provide evidence for an enhanced bioavailability. This would promote the use of phytoremediation as a technique for removing hydrophobic organic contaminants.

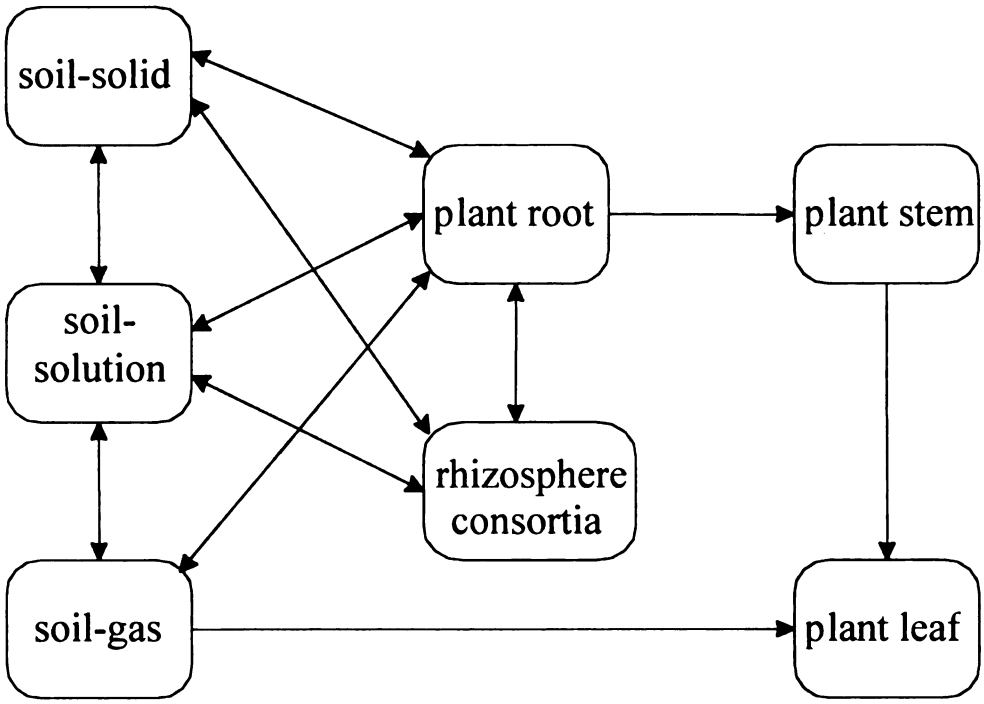

Figure 2-1. A simplified diagram that shows some of the interactions that occur in planted systems.

Table 2-1. Types of phytoremediation (adapted from McCutcheon and Schnoor[65])

Type	Definition	Current use or potential use
phytodegradation	the degradation or transformation of organic contaminants to less toxic forms by plants	chlorinated solvents, PCBs, energetic materials, Cl and P based pesticides
phytostimulation	the supply of a carbon source by exudation, secretion and root necrosis that stimulates enzyme induction or cometabolism by soil microbes	organic compounds, e.g. BTEX, TPH, PAHs, PCBs, pesticides, etc.
phytostabilization	stabilization of contaminants by inhibiting soil erosion, promoting precipitation, enhancing sorption, or causing irreversible binding of contaminants to soil	metals, phenols, chlorinated solvents
phytocontainment	the hydraulic control of contaminants using plants to transpire large amounts of water, thus minimizing contaminant leaching	water soluble contaminants such as MTBE, chlorinated solvents and energetic materials
phytovolatilization	volatile metals are taken up in the transpiration stream and transpired	Se, As, Hg, chlorinated solvents
Phytoextraction	contaminant uptake with the transpiration stream and transport to the aerial tissues; hyperaccumulation occurs when the compound or element exceeds 100 times its normal concentration in the plant	metals, radionuclides, relatively soluble organic compounds

References

1. Cunningham, S.D. and W.R. Berti, *Remediation of contaminated soils with green plants: an overview.* In Vitro Cellular and Developmental Biology, 1993. **29**: p. 207-212.

2. Schnoor, J.L., et al., *Phytoremediation of organic and nutrient contaminants.* Environmental Science and Technology, 1995. **29**(7): p. 318A-323A.

3. Schwab, A.P., A.A. Al-Assi, and M.K. Banks, *Plant and environment interactions: adsorption of naphthalene onto plant roots.* Journal of Environmental Quality, 1998. **27**: p. 220-224.

4. Newman, L., et al., *Phytoremediation of organic contaminants: A review of phytoremediation research at the University of Washington.* Journal of Soil Contamination, 1998. **7**: p. 531-542.

5. Barac, T., et al., *Engineered endophytic bacteria improve phytoremediation of water-soluble, volatile, organic pollutants.* Nature Biotechnology, 2004. **22**: p. 583-588.

6. White, J.C., et al., *Role of organic acids in enhancing the desorption and uptake of weathered p,p'-DDE by Cucurbita pepo.* Environmental Pollution, 2003. **124**: p. 71-80.

7. Sung, K., et al., *Plant contamination by organic pollutants in phytoremediation.* Environmental Quality, 2001. **30**: p. 2081-2090.

8. Huang, X., et al., *A multi-process phytoremediation system for removal of polycyclic aromatic hydrocarbons from contaminated soils.* Environmental Pollution, 2004: p. 2-12.

9. Alkorta, I. and C. Garbisu, *Phytoremediation of organic contaminants in soils.* Bioresource Technology, 2001. **79**: p. 273-276.

10. Chekol, T., L. Vough, and R.L. Chaney, *Plant-soil-contaminant specificity affects phytoremediation of organic contaminants.* International Journal of Phytoremediation, 2002. **4**(1): p. 17-26.

11. Gao, Y., L. Zhu, and W. Ling, *Application of the partition-limited model for plant untake of organic chemicals from soil and water.* Science of the Total Environment, 2004.

12. Sidolio'Connor, C., N. Lepp, and G. Sunderland, *The combines use of electrokinetic remediation and phytoremediation to decontaminate metal-polluted soil: a laboratory-scale feasibility study.* Environmental Monitoring and Assessment, 2003. **84**: p. 141-158.

13. Gremion, F., et al., *Impacts of heavy metal contamination and phytoremediation on a microbial community during a twelve month microcosm experiment.* FEMS Microbiology Ecology, 2004. **48**: p. 273-283.

14. Podar, D., M. Ramsey, and M. Hutchings, *Effect of cadmium, zinc and substrate heterogeneity on yirld, shoot metal concentration and metal uptake by Brassica juncea: implications for human health risk assessment and phytoremediation.* New Phytologist, 2004. **163**: p. 313-324.

15. Meharg, A.A. and L. Jardine, *Arsenite transport into paddy rice (Otyza sativa) roots.* New Phytologist, 2003. **157**: p. 39-44.

16. Leonard, T., et al., *Mercury and plants in contaminated soils: 1. uptake, partitioning, and emission to the atmosphere.* Environmental Toxicology and Chemistry, 1998. **17**(10): p. 2063-2071.

17. Gong, J.-M., D.A. Lee, and J.I. Schroeder, *Long-distance root-to-shoot transport of phytochelatins and cadmium in arabidopsis.* PNAS, 2003. **100**(17): p. 10118-10123.

18. Absalom, J.P., et al., *Predicting soil to plant transfer of radiocesium using soil characteristics.* Environmental Science and Technology, 1999. **33**: p. 1218-1223.

19. Huang, J.W., et al., *Phytoremediation of uranium-contaminated soils: role of organic acids in triggering uranium hyperaccumulation in plants.* Environmental Science and Technology, 1998. **32**: p. 2004-2008.

20. Newman, L., et al., *Uptake and biotransformation of trichloroethylene by hybrid polars.* Environmental Science and Technology, 1997. **31**: p. 1062-1067.

21. Goel, A., et al., *Plant cell biodegradation of a xenobiotic nitrate ester, nitroglycerin.* Nature Biotechnology, 1997. **15**: p. 174-177.

22. Van Aken, B., J.M. Yoon, and J.L. Schnoor, *Biodegradation of nitro-substituted explosives 2,4,6-trinitrotoluene, hexahydro-1,3,5-trinitro-1,3,5-triazine, and octahydro-1,3,5,7-tetranitro-1,3,5-tetrazocine by a phytosymbiotic Methylobacterium sp. associated with Poplar tissues(Populus deltoides X nigra DN34).* Applied and Environmental Microbiology, 2003. **70**(1): p. 508-517.

23. Banks, M.K., et al., *Degradation of crude oil in the rhizosphere of Sorghum bicolor.* International Journal of Phytoremediation, 2003. **5**(3): p. 225-234.

24. Burken, J.G. and J.L. Schnoor, *Phytoremediation: plant uptake of atrazine and role of root exudates.* Journal of Environmental Engineering, 1996. **122**(11): p. 958-963.

25. Ferro, A.M., R.C. Sims, and B. Bugbee, *Hycrest crested wheatgrass accelerates the degradation of pentachlorophenol in soil.* Journal of Environmental Quality, 1994. **23**: p. 272-279.

26. Hedge, R.S. and J.S. Fletcher, *Influence of Plant Growth Stage and Season on the Release of Root Phenolics by Mulberry as Related to Development of Phytoremediation Technology.* Chemosphere, 1996. **32**(12): p. 2471-2479.

27. Kamath, R., J. Schnoor, and P. Alvarez, *Effect of root-derived substrates on the expression of nah-lux genes in Pseudomonas fluorescens HK44: Implications for PAH Biodegradation in the Rhizosphere.* Environmental Science and Technology, 2004. **38**: p. 1740-1745.

28. Salt, D.E., R.D. Smith, and I. Raskin, *Phytoremediation.* Annual Review of Plant Physiology and Plant Molecular Biology, 1998. **49**: p. 643-668.

29. Matthews, D.W., J. Massmann, and S.E. Strand, *Influence of aquifer properties on phytoremediation effectiveness.* Ground Water, 2003. **41**(1): p. 41-47.

30. Ma, X., et al., *Phytoremediation of MTBE with hybrid poplar trees.* International Journal of Phytoremediation, 2004. **6**(2): p. 157-167.

31. Dushenkov, S., *Trends in phytoremediation of radionuclides.* Plant and Soil, 2003. **249**(1): p. 167-175.

32. Curl, E.A. and B. Truelove, *The Rhizosphere.* 1986: Springer-Verlag Berlin Heidelberg.

33. Waisel, Y., A. Eshel, and U. Kafkafi, eds. *Plant Roots: The Hidden Half.* 2002, Marcel Dekker, Inc.: New York City. 1120.

34. Lynch, J.M., ed. *The Rhizosphere.* 1990, John Wiley and Sons, Inc.: New York City.

35. Siciliano, S.D. and J.J. Germida, *Bacterial inoculants of forage grasses that enhance degradation of 2-chlorobenzoic acid in soil.* Environmental Toxicology and Chemistry, 1997. **16**(6): p. 1098-1104.

36. Jordahl, J., et al., *Effect of hybrid poplar trees on microbial populations important to hazardous waste bioremediation.* Environmental Toxicology and Chemistry, 1997. **16**: p. 1318-1321.

37. Jones, D., *Organic acids in the rhizosphere - a critical review.* Plant and Soil, 1998. **205**: p. 25-44.

38. Hillel, D., *Environmental Soil Physics.* 1998, San Diego: Academic Press.

39. Stevenson, F.J., *Humus Chemistry: Genesis, Composition, Reactions*. 2 ed. 1994: John Wiley and Sons, Inc.

40. Thibodeaux, L.J., *Environmental Chemodynamics*. 1996, New York City: John Wiley and Sons, Inc. 593.

41. Schwarzenbach, R.P., P.M. Gschwend, and D.M. Imboden, *Environmental Organic Chemistry*. 2nd ed. 2003, Hoboken: John Wiley and Sons, Inc.

42. Connaughton, D.F., et al., *Description of time-varying desorption kinetics: release of naphthalene from contaminated soils.* Environmental Science and Technology, 1993. **27**: p. 2397-2403.

43. Harmon, T.C. and P.V. Roberts, *Comparison of intraparticle sorption and desorption rates for a halogenated alkene in a sandy aquifer material.* Environmental Science and Technology, 1994. **28**: p. 1650-1660.

44. Johnson, M.D. and J. Weber, W.J., *Rapid prediction of long-term rates of contaminant desorption from soils and sediments.* Environmental Science and Technology, 2001. **35**: p. 427-433.

45. Lesan, H.M. and A. Bhandari, *Atrazine sorption on surface soils: time-dependent phase distribution and apparent desorption hystersis.* Water Research, 2003. **37**: p. 1644-1654.

46. Sharer, M., et al., *Time dependence of chlorobenzene sorption/desorption by soils.* Soil Science Society of Americal Journal, 2003. **67**: p. 1740-1745.

47. Ahn, I.-S., L.W. Lion, and M.L. Shuler, *Validation of a hybrid "two-site gamma" model for naphthalene desorption kinetics.* Environmental Science and Technology, 1999. **33**: p. 3241-3248.

48. Bayard, B., et al., *Investigation of naphthalene in soils and soil fractions using batch and column assays.* Environmental Toxicology and Chemistry, 1998. **17**(12): p. 2383-2390.

49. Cornelissen, G., P.C.M. van Noort, and H.A.J. Govers, *Mechanism of slow desorption of organic compounds from sediments: A study using model sorbents.* Environmental Science and Technology, 1998. **32**: p. 3125-3131.

50. Park, J.-H., X. Zhao, and T.C. Voice, *Development of a kinetic basis for bioavailability of sorbed naphthalene in soil slurries.* Water Research, 2002. **36**: p. 1620-1628.

51. Tabak, H.H., et al. *Determination of bioavailability and biodegradation kinetics of polycyclic aromatic hydrocarbons in soil.* in *Emerging Technologies in Hazardous Waste Management*. 1995.

52. Park, J.-H., et al., *Kinetic modeling of bioavailability for sorbed-phase 2,4-dichlorophenoxyacetic acid.* Journal of Environmental Quality, 2001. **30**: p. 1523-1527.

53. Brusseau, M.L., R.E. Jessup, and P.S.C. Rao, *Modeling the transport of solutes influenced by multiprocess nonequilibrium.* Water Resources Research, 1989. **25**(9): p. 1971-1988.

54. Siciliano, S.D. and J.J. Germida, *Mechanisms of phytoremediation: biochemical and ecological interactions between plants and bacteria.* Environmental Reviews, 1998. **6**: p. 65-79.

55. Fletcher, J.S. and R.S. Hegde, *Release of phenols by perennial plant roots and their potential importance in bioremediation.* Chemosphere, 1995. **31**(4): p. 3009-3016.

56. Rentz, J., P. Alvarez, and J. Schnoor, *Repression of Pseudomonas putida phenanthrene-degrading activity by plant root extracts and exudates.* Environmental Microbiology, 2004. **6**: p. 574-583.

57. Hopkins, W.G., *Introduction to Plant Physiology.* 1995: John Wiley and Sons, Inc.

58. Briggs, G.G., R.H. Bromilow, and A.A. Evans, *Relationships between lipophilicity and root uptake and translocation of non-ionised chemicals in barley.* Pesticide Science, 1982. **13**: p. 495-504.

59. Burken, J.G. and J.L. Schnoor, *Predictive relationships for uptake of organic contaminants by hybrid poplar trees.* Environmental Science and Technology, 1998. **32**: p. 3379-3385.

60. Millington, R. and J. Quirk, *Permeability of porous solids.* Transactions of the Faraday Society, 1961. **57**: p. 1200-1207.

61. Freeze, R.A. and J.A. Cherry, *Groundwater.* 1979: Prentice-Hall, Inc.

62. Davis, L.C., et al., *Modeling the effects of plants on the bioremediation of contaminated soil and ground water.* Environmetanl Progress, 1993. **12**(1): p. 67-75.

63. Davis, L.C., et al., *Benefits of vegetation for soils with organic contaminants.* Critical Reviews in Plant Sciences, 2002. **21**: p. 457-491.

64. Chang, Y.Y. and M.Y. Corapcioglu, *Plant-enhanced subsurface bioremediation of nonvolatile hydrocarbons.* Journal of Environmental Engineering, 1998. **124**(2): p. 162-169.

65. McCutcheon, S.C. and J.L. Schnoor, *Overview of phytotransformation and control of wastes*, in *Phytoremediation: Transformation and Control of*

Contaminants, S.C. McCutcheon and J.L. Schnoor, Editors. 2003, John Wiley and Sons, Inc.: Hoboken, New Jersey. p. 3-58.

Chapter 3. Describing HOC desorption profiles exhibiting distinct observational regimes

Abstract

Desorption of organic contaminants from soil can be modeled by dividing the desorption profile into three distinct regimes. These are an instantaneous (i.e. too fast to measure) desorbing regime, a nonequilibrium (i.e. slow enough to measure) desorbing regime, and a desorption-resistant (i.e. a non-desorbing) regime. Batch desorption curves for atrazine and naphthalene on four soils were experimentally generated to demonstrate the existence of discrete observational regimes. Nine mathematical models, each containing mechanisms formulated to describe at least one of the three regimes, were fit to each contaminant-soil combination using the Gauss-Newton method for parameter estimation. Each of the nine models was ranked using the small-sample corrected Akaike information criterion (AICc). By interpretation of the AICc values, the atrazine desorption data was best described by three behavioral regimes. Mechanisms for fast, slow and non-desorption were justified by the gathered data. However, AICc values often justified the inclusion of only two regimes for naphthalene desorption data. Estimation of an equilibrium fraction was not justified by the data because of increased model variability, whereas models that contain slow and non-desorption mechanisms were justified by the data. This is a result of the sparse number of data points in the slow regime—therefore, only nonequilibrium and non-desorptive regimes are justified in describing the data.

Introduction

Rationale and scope for the present study

There is widespread evidence from the field that hydrophobic organic contaminant remediation is often limited by desorption. Desorption can be a limiting factor for a number of remediation technologies, including: microbial bioremediation, phytoremediation, landfarming, and pump and treat[1]. Models that accurately predict desorption phenomena at long times are needed for design of site clean up, as desorption is often regarded as the first step in remediation. Though in some cases the risk associated with slow contaminant desorption may be deemed acceptable and requiring no remediative action[2, 3], it remains important to accurately predict the amount of contaminant sorbed to the soil using a descriptive model. Several researchers have suggested that contaminant desorption profiles can be divided into distinct regimes, predicated on fast, slow, and very slow desorption behavior. Several models have been formulated with the necessary descriptive power to quantify contaminant transport within these regimes. Though the magnitude of desorption is important for remediation design, few models adequately describe desorption profiles in the very slow or non-desorption regime.

Review of desorption data

It is widely accepted that contaminant desorption in situ may consist of a fast regime, occurring at a rate too quick to measure, a dynamic regime, occurring at a rate that can be measured, and a slow regime occurring at a rate too slow to measure. Fast and slow desorption have been witnessed by a number of researchers. However,

contaminant desorption witnessed on-site is often very slow and frequently not measurable, due to the microscale processes of sequestration[4]. An estimate of the amount of contaminant sorbed to this very slowly desorbing fraction can be determined via simple lab assays (i.e. desorption experiments). These desorption experiments are typically conducted over time spans ranging from hours to months and the resultant contaminant desorption profiles have been presented in the literature[5-11].

Review of modeling literature

Relatively few models include mechanisms to describe all three types of observations (i.e. fast, slow and very slow desorption). However, rarely does observed desorption of organic contaminants from soils reach one hundred percent, hence the need to adequately describe slow and very slow desorption. As a significant fraction of the contaminant remains sorbed to the soil in a recalcitrant manner, it has been hypothesized that contaminants displaying this type of behavior are sorbed to non-desorption[11], desorption-resistant[12], or irreversible[1] binding fractions of the soil organic matter. The rate of desorption from these fractions is a function of the quantity and quality of the soil organic matter[5]. Several models have been formulated to predict organic contaminant desorption though few accurately and precisely describe desorption at long times. The chemical two and three-site models presume that a nonequilibrium desorption reaction explains the behavior of organic contaminants in soil matrices[13]. The chemical two-site model is not formulated to describe non-desorption, while the chemical three-site model contains an added mathematical compartment specifically for non-desorption. The physical one[14], two and three-parameter pore-diffusion models explain contaminant transport through soil particles using Fickian diffusive flux terms.

The one-parameter pore diffusion model cannot predict instantaneous desorption or desorption at long time scales. Both the two-parameter pore diffusion model and the three-parameter pore diffusion model can predict instantaneous desorption; though only the three-parameter pore diffusion model can describe the desorption profile in the non-desorption regime. Models based on the gamma distribution function abstractly partition the soil into a number of mathematical domains, with each domain having a different mass transfer coefficient[15]. The gamma model is not formulated to predict instantaneous desorption while the hybrid gamma/two-site model contains a mechanism allowing for equilibrium (instantaneous desorption) between the solid and liquid phases[16]. These models can describe desorption at long times though both are somewhat arduous to solve. Three and five-parameter kinetic models have also been developed to more adequately reflect desorption behavior[7, 9]. These models are simple in formulation, though mathematical convergence of parameter estimation algorithms applied to desorption data with a significant non-desorption regime can be problematic.

Comparison of this approach with previous attempts at model selection

A number of models may be used to describe the contaminant desorption profile, as the limiting mechanism involved in contaminant desorption is likely system-specific. This work focuses on comparing these various models using atrazine and naphthalene desorption data that was gathered from four soils. Previously, Johnson et al[17] have compared six models using phenanthrene desorption data from three different soils. They concluded that desorption profiles are at least biphasic and that models composed of two regimes are good starting points for describing desorption. They further concluded that model selection is system-specific, as the apparent desorption rate is likely

a function of different rate-limiting mechanisms from one soil-contaminant combination to the next. The effort presented in this article extends Johnson's findings by surveying desorption data that can likely be described by models composed of three regimes. Furthermore, this study uses the Akaike information criterion (AIC) for the purpose of model ranking and model selection. The AIC couples the information inherent in the data with the model formulations to optimize the balance of model accuracy and model variability. This technique was applied to atrazine and naphthalene desorption profiles to investigate the types of desorption data that justify the use of a two-regime models and the types that justify three-regime models. Comparisons were also made amongst four soil types to determine the effect the soil matrix has on the selection of two- or three-regime models for a given contaminant. To investigate the effect that model structure has on model selection, several different two- and three-regime models were included in this study. Ultimately, in the case that contaminant desorption from several soils is best described by a single model, this model becomes more than a mere description of the data—it becomes an explanation for the data, or theory.

Methods and Mathematics

Contaminant desorption profiles, demonstrating the existence of distinct behavioral regimes, were generated for both contaminants in four soils. The four soils used in this study were: Hartsells, Capac A, Colwood A and Houghton muck. Soils were air dried, ground, and passed through a 2-mm sieve. Soil organic carbon contents and particle size distribution were determined by the Soil and Plant Nutrient Laboratory at Michigan State University. Table 3-1 summarizes the properties of the soils. Soil samples were sterilized by γ-irradiation (1.29 Mrad/hr, 5 Mrad from a ^{60}Co source) and stored in sealed containers at room temperature. Before each experiment using soils, 0.1 g of each soil was placed on a half-strength nutrient agar plate and incubated at 30 °C for 3 days to verify sterility. No colony-forming units (CFU) were observed.

The desorption profiles were constructed using a batch apparatus and spiking the soil and water mixture with ^{14}C labeled atrazine and naphthalene. Atrazine or naphthalene was spiked into each of these soils to observe desorption. The desorption assay of naphthalene utilized batch soil slurries. An aliquot of ^{14}C-naphthalene stock (in methanol, 7.5 g/L) was spiked into 25 mL centrifuge tubes containing 24 mL of sterile phosphate buffer (20 mM) and each sterile soil (1.5 g of Hartsells, 1.3 g of Capac, 0.3 g of Colwood, and 0.3 g of Houghton muck) to get 2 mg/L of initial aqueous naphthalene concentration. The tubes were capped with a Teflon-lined Mininert® valve and screw-sealed with polypropylene caps. A control tube without soil was prepared in the same fashion. Tubes were tumbled at 9 rpm for 2 days in the dark, then each tube was centrifuged for 20 min at 1200 g to separate soil, and the supernatant was sampled. The final concentration of naphthalene in the liquid phase was determined by liquid

scintillation counting (LSC), and the amount of sorbed naphthalene was calculated by difference. The supernatant was then decanted to the extent possible, and the residual water determined gravimetrically. Desorption was initiated by adding fresh naphthalene-free soil-extract to make-up the original volume. The tubes were tumbled again at 9 rpm, then removed periodically and the liquid phase sampled for analysis by LSC. Samples were initially taken at one-hour increments as this is the most dynamic regime in the desorption profile. As the desorption profile appeared to enter the non-desorptive regime, the time increment between samples was increased. The entire desorption profile was collected over a period of three days. The concentration of naphthalene in the final desorption samples were determined by LSC and verified with high-performance liquid chromatography (HPLC). After the final desorption samples, the soil was separated from the supernatant and extracted with methanol. The concentration of naphthalene in the extracts was determined by LSC and verified with HPLC.

The models presented in Table 3-2 were formulated to describe the resultant desorption data. The chemical three-site model was constructed to model irreversible desorption[11, 18, 19]. This model contains a reversible regime, described using local equilibrium; a nonequilibrium regime, parameterized by a desorption rate coefficient; and a non-desorption regime, used to accurately model irreversible desorption profiles. The chemical two-site model is not formulated to describe the non-desorptive (or irreversible) regime of the desorption profile, but is formulated with an equilibrium and a nonequilibrium compartment[20-23]. The three-parameter pore diffusion model is formulated using a reversible regime, described using local equilibrium; a nonequilibrium regime, parameterized by an apparent diffusion coefficient; and a non-desorption regime,

used to accurately model irreversible desorption profiles. This model has not been previously presented in the literature. The two-parameter pore diffusion model[17] is not formulated to model the non-desorptive regime of the desorption profile, but is formulated with an equilibrium and a diffusion limited compartment. The one-parameter pore diffusion model[6, 10, 14, 24-26] only contains a diffusive compartment, and cannot model instantaneous desorption or non-desorption. The gamma distribution model[15] uses a gamma distribution function to mathematically partition the soil into a number of distinct fractions. This model is strictly empirical as it is parameterized by two coefficients, α and β. Neither of these parameters has an easily discernable physical meaning. The hybrid gamma/two-site model[16] assumes that the desorption from each of the sites, assigned by the gamma distribution function, proceeds in the same manner as that would occur in the chemical two site model. The added parameter, f_{eq}, improves the model accuracy for describing certain desorption profiles. Both gamma distribution models were somewhat cumbersome to program and interpret. The five-parameter kinetic model[7, 9, 17] consisted of a fast desorption regime, a slow desorption regime and a very slow desorption regime. Each regime is quantified using first order kinetics and the resultant solution is a summation of exponentials. This model was difficult to solve as the very slow regime kinetic constant converges to a value near zero. Application of this model to the data in this article proceeded by equating the accumulation rate for this fraction to zero. Thus a modified five-parameter kinetic model only uses four parameters. The three-parameter kinetic model[8, 9, 27, 28] is similar to the five-parameter model with the exception that it does not contain a very slow compartment. Again, in order to provide convergence, the slow compartment

accumulation rate was set to zero, and the modified three-parameter kinetic model only uses two parameters.

Each of the models presented in Table 3-2 was solved analytically or numerically for the purpose of parameter estimation. All of the solutions were programmed using the Matlab software package and the output was generated using Matlab's graphical user interface. The error sum of squares between the data and the model fits were used as objective functions for parameter estimation. These objective functions were minimized using the Gauss-Newton method assuming a tolerance of 10^{-3} as the convergence criterion[29]. A modified version of the Gauss-Newton method was used for problems where the dependent variables were nonlinearly related to the independent variables, such as for the gamma and hybrid gamma/two-site models. Stiffness was overcome for both the gamma distribution and hybrid gamma distribution models by using reduced sensitivity coefficients. Parameter standard errors were estimated from the resultant sensitivity matrix.

Model inference was accomplished through application of the Akaike information criterion (AIC)[30, 31]. This criterion uses estimates of accuracy and precision as a means of model inference and subsequent selection. The ranking of models based on accuracy alone is not sufficient because model variability is not included. Akaike formulated the AIC by noticing a relationship between the Kullback-Leibler distance and the maximized log-likelihood function. The leftmost term on the right-hand side of equation 3-1 represents a penalty for under-fitting data and the right term is a penalty for over-fitting data.

$$AIC = n\log(\hat{\sigma}^2) + 2K \qquad \text{(Equation 3-1)}$$

The AIC tells what inferences the data support, not what reality might be. In a sense, the AIC is a quantitative Occam's razor (a rule that states that the simplest of competing descriptions is preferred) that can be used to select the most parsimonious model supported by the collected data. The principle of parsimony insists that the best-fit model is the model with an optimal combination of bias and variability (contrary to R^2, which only determines goodness of fit based on accuracy alone). Because the AIC is the sum of two penalty terms (i.e. one for bias and one for uncertainty), the smaller AIC values correspond to models that fit the data more parsimoniously. Models are then ranked according to each AIC value.

The small-sample corrected AIC—given the acronym AIC_c (equation 3-2), is used in this study, as warranted by the small sample size relative to the number of model parameters.

$$AIC_c = AIC + \frac{2K(K+1)}{n-K-1} \qquad \text{(Equation 3-2)}$$

The nine models chosen for this inquiry were ranked for each soil-contaminant combination using the value of the AICc.

Results and Discussion

Desorption data for Capac A-atrazine and Muck-naphthalene were fit with nine mathematical models using the Gauss-Newton technique. Eight of the nine models are presented in Figure 3-1 (Capac A-atrazine) and Figure 3-2 (Muck-naphthalene). Note that the atrazine profile approaches the maximum desorbed amount in a more gradual manner than does naphthalene profile. Therefore, there are more data points in the dynamic region of the atrazine desorption profile than in naphthalene desorption profile. Consequently, the atrazine data supports the inclusion of an equilibrium site in the model formulations, whereas the naphthalene data does not support the inclusion of an equilibrium site. The details of each soil-contaminant combination are described and discussed in the following sections.

Capac A

The AICc values for Capac A soil are presented in Figure 3-3 for both atrazine and naphthalene. Increasing the number of regimes is beneficial for atrazine desorption from Capac A, and the desorption data is best described by the chemical three-site model. The three-regime models that contain an equilibrium site—such as the chemical three-site model, the three-parameter pore diffusion model, and the hybrid gamma/two-site model—are favorable to the three-regime model that does not include and equilibrium site, namely the five parameter kinetic model. Likewise, the two-regime models that contain an equilibrium site—such as the chemical two-site and the two-parameter pore diffusion models, are better formulated for describing Capac A-atrazine desorption data when compared to the models that do not contain an equilibrium site, namely the gamma

and the three-parameter kinetic models. Unlike the model ranking for the three-regime models, the two-parameter pore diffusion model provides the best description amongst the two-regime models, as the two-parameter pore diffusion model is more capable of handling curvature than is the chemical two-site model. The one-parameter pore diffusion provides a poor description of Capac A-atrazine desorption data.

As with the Capac A-atrazine data, the Capac A-naphthalene data warrant an additional regime in the chemical site and the pore diffusion models (Figure 3-4). The chemical three-site and the three-parameter pore diffusion models provide superior descriptions of the Capac A-naphthalene data than do the chemical two-site and the two-parameter pore diffusion models, respectively. Contrary to the Capac A-atrazine data, the Capac A-naphthalene data does not warrant an additional regime for the gamma and kinetic models. Adding an equilibrium site to the gamma model to form the hybrid gamma/two-site model does not improve the gamma model's description of the Capac A-naphthalene data. This is a result of the sparseness of the data at short desorption times for the Capac A-naphthalene desorption profiles. In other words, there is a lesser amount of data in the curved portion of the desorption profile for Capac A-naphthalene than for the Capac A-atrazine, and therefore the ability to estimate an equilibrium site fraction is negatively impacted. The additional parameters, used to formulate the five-parameter kinetic model from the three-parameter kinetic model, are not justified by the data. Also, converse to the Capac A-atrazine data, the Capac A-naphthalene is best described by a two-regime model, namely the three-parameter kinetic model. Again the sparseness of data in the early portion of the desorption profile negates the inclusion of an equilibrium site fraction, a fraction that is not present in the three-parameter kinetic model. The

accuracy gained by addition of a further desorption regime is not significant compared to the added parameter uncertainty.

Colwood A

The Colwood A-atrazine data follows the same trend as the Capac A-atrazine data—specifically, the three-regime models provide better descriptions of the data than the two-regime models (Figure 3-5). Again, the chemical three-site model provides the best description of the data. The two-regime models that can adequately model curvature in the desorption profile, such as the two-parameter pore diffusion and the gamma models, are superior to those that cannot, namely the chemical two-site model.

The Colwood A-naphthalene data is best modeled by the two-parameter pore diffusion model and the gamma model (Figure 3-6). In the case of the pore diffusion models, adding a regime does not change the AICc value, and in the case of the gamma family of models, the addition of an equilibrium site fraction does not improve the description of the data. Converse to the Capac A-naphthalene data, the kinetic models are improved by the addition of a regime. Like Capac A-naphthalene, the two-regime models provide the best description of the Colwood A-naphthalene desorption profile.

Hartsells

The Hartsells-atrazine data is best described by the three-regime models (Figure 3-7), as with Capac A-atrazine and Colwood A-atrazine. Again, the chemical three-site model provides the best description of the desorption profile. Of the two-regime models, the two-parameter pore diffusion model provides the best description of the Hartsells-

atrazine desorption profile. The one-parameter pore diffusion model is a poor description of the Hartsells-atrazine data.

The Hartsells-naphthalene data follows the same trend as the Capac A-naphthalene data (Figure 3-8). For the chemical site and pore diffusion models, increasing the number of regimes provides a superior description of the data. However, the converse is true for the gamma and kinetic models. As with Capac A-naphthalene, the gamma and the three-parameter kinetic models provide the best description of the Hartsells-naphthalene desorption profiles, a consequence of the sparseness of early desorption data and the lack of improved fit, respectively.

Muck

The Muck-atrazine data is best described by the three-regime models (Figure 3-9), as with Capac A-atrazine, Colwood A-atrazine, and Hartsells-atrazine. Again, the chemical three-site model provides the best description of the desorption profile. Unlike Capac A-atrazine, Colwood A-atrazine, and Hartsells-atrazine, the gamma model is the best two-regime model for describing Muck-atrazine desorption data. The one-parameter pore diffusion model is a poor description of the Muck-atrazine data.

Of note is the sparseness of data in the curved portion of the profile. The Muck-naphthalene data follows the same trend as the Capac A-naphthalene and Hartsells-naphthalene data (Figure 3-10). For the chemical site and pore diffusion models, increasing the number of regimes provides a superior description of the data. However, the converse is true for the gamma and kinetic models. As with Capac A-naphthalene and Hartsells-naphthalene, the gamma and the three-parameter kinetic models provide the

best description of the Muck-naphthalene desorption profiles, a consequence of the sparseness of early desorption data and the lack of improved fit, respectively.

Discussion of contaminants

Atrazine desorption data tends to be well described by models in the three-regime category. In all cases, increasing the number of parameters is justified by the decrease in the AICc value. Of the three regime models, the chemical three-site model tends to provide the best description of the data. Further benefits from using the chemical three-site model are: 1) the relative ease of programming and 2) the relative ease of interpreting the values of the estimated parameters. Of the three-regime models, the modified five-parameter kinetic model provides the worst fit of the data. The five-paramenter kinetic model lacks an equilibrium compartment, and is therefore unable to accurately describe the early portion of the desorption data. Of the two-regime models, the gamma model provides the best fit of the data. This model is better formulated to describe the intermediate and late portions of the desorption data, as it is capable of more accurately fitting the curvature present in the desorption profile. The one-parameter pore diffusion model does not accurately describe the desorption data, as it is not formulated to describe the early and late portions of the desorption profile.

The naphthalene desorption data provides an exception to the conclusions drawn from the atrazine desorption data. The gamma model tends to be justified by the data over the three-regime models. This is a result of the gamma model's ability to describe curvature in the intermediate and late portions of the desorption profile, and the nature of the naphthalene desorption data. Relatively few data points are collected during the early desorption profile as naphthalene desorption rapidly approaches the maximum fraction

desorbed. Models with an equilibrium compartment are not as justified for naphthalene as for atrazine, because the estimation of the equilibrium compartment size is based on a small number of data points. Therefore, a model that is capable of describing the intermediate and the late portions of the desorption profile—while not making estimates of an equilibrium compartment based on sparse data—will tend to have a lower AICc value. As such, the reformulation of the gamma model to include an equilibrium compartment, i.e. the hybrid gamma/two-site model, is not justified. Accuracy in predicting the intermediate and the late portions of the desorption profile is still justified, as the chemical three-site and the three-parameter pore diffusion models remain good descriptors of these types of desorption profiles.

Discussion of models

The three regime-models fit the atrazine data better than the two-regime models. For the chemical site models, the pore diffusion models, and the kinetic models, the additional parameters provide an improved fit to the data. For the gamma models, the fact that the additional parameterization involves an equilibrium site fraction that is justified by the nature of the early portion of the atrazine desorption profiles is an added benefit. Of the two regime models, the two-parameter pore diffusion and the gamma models tend to provide the best description of the data, a result of each model's ability to fit curvature compared with the other two regime models. For naphthalene, the gamma and the three-parameter kinetic models provide the best description of the desorption profiles. This is an artifact of the sparseness of the early desorption data which leads to an inability to precisely determine the equilibrium site fraction. Finally, the one-parameter pore diffusion model consistently provides the poorest description of the

desorption data, as it predicts a lower desorbed fraction at early times, and greater desorbed fractions at longer times.

Conclusions

For desorption data exhibiting profiles reminiscent of atrazine desorption, the chemical three-site model provides the best description of the data. For desorption data exhibiting profiles reminiscent of naphthalene desorption, the gamma and the three-parameter kinetic models provide the best descriptions of the data. The three-parameter kinetic model is recommended over the gamma model, because of the relative ease involved in formulation and subsequent interpretation of estimated parameters.

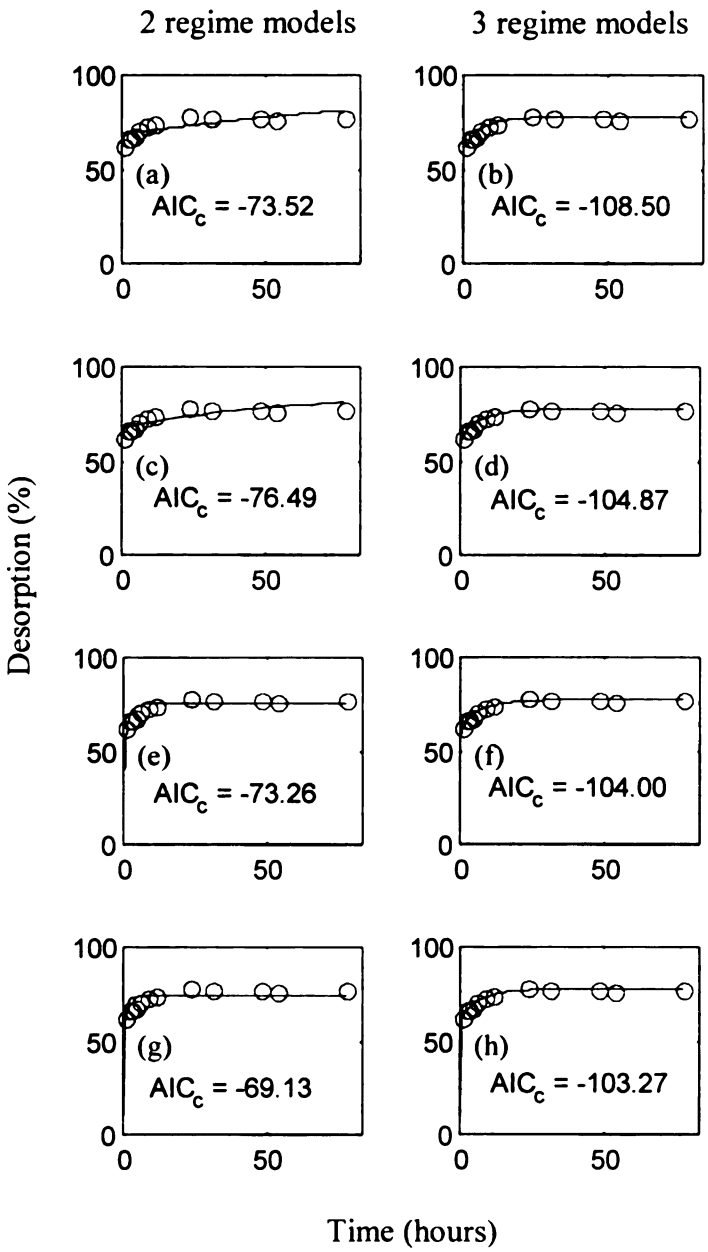

Figure 3-1. Best-fit models to atrazine-Capac A desorption data: (a) the chemical two-site model, (b) the chemical three-site model, (c) the two-parameter pore diffusion model, (d) the three-parameter pore diffusion model, (e) the gamma model, (f) the hybrid gamma/two-site model, (g) the modified three-parameter kinetic model and (h) the modified five-parameter kinetic model.

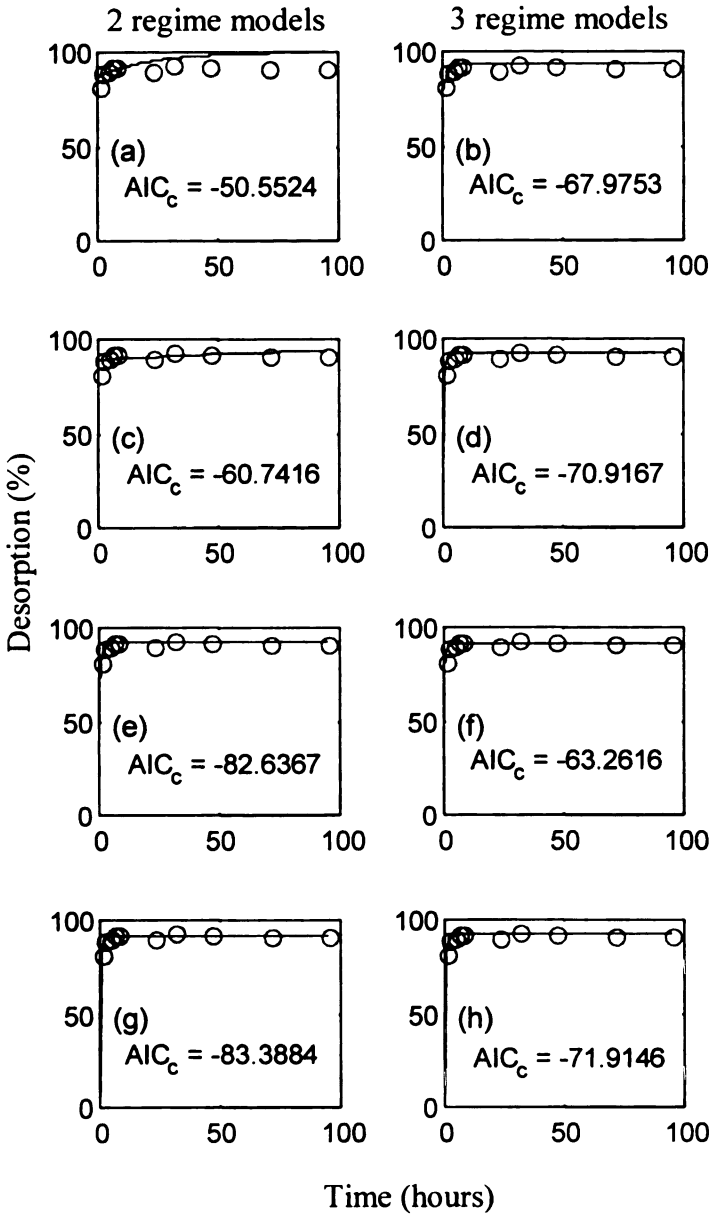

Figure 3-2. Best-fit models to naphthalene-Muck desorption data: (a) the chemical two-site model, (b) the chemical three-site model, (c) the two-parameter pore diffusion model, (d) the three-parameter pore diffusion model, (e) the gamma model, (f) the hybrid gamma/two-site model, (g) the modified three-parameter kinetic model and (h) the modified five-parameter kinetic model.

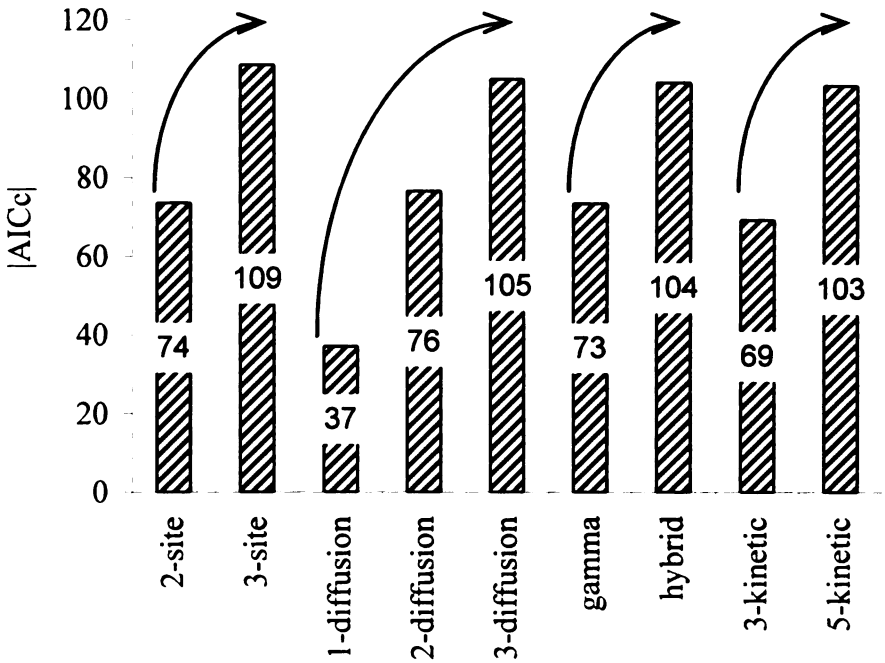

Figure 3-3. Comparison of the AICc for the nine models that were fit to Capac A-atrazine desorption data.

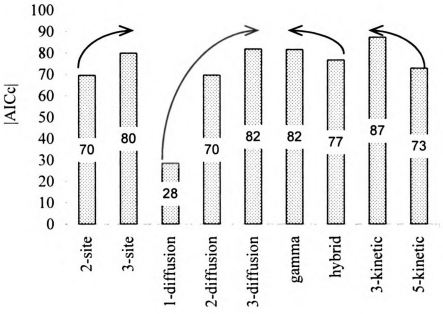

Figure 3-4. Comparison of the AICc for the nine models that were fit to Capac A-naphthalene desorption data.

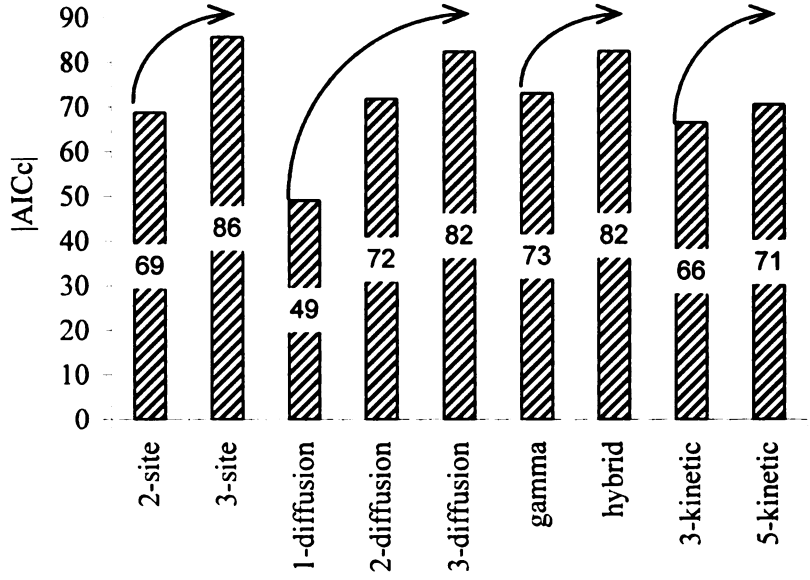

Figure 3-5. Comparison of the AICc for the nine models that were fit to Colwood A-atrazine desorption data.

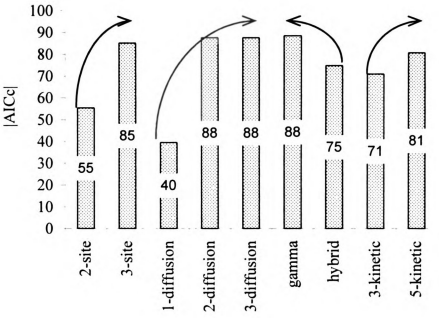

Figure 3-6. Comparison of the AICc for the nine models that were fit to Colwood A-naphthalene desorption data.

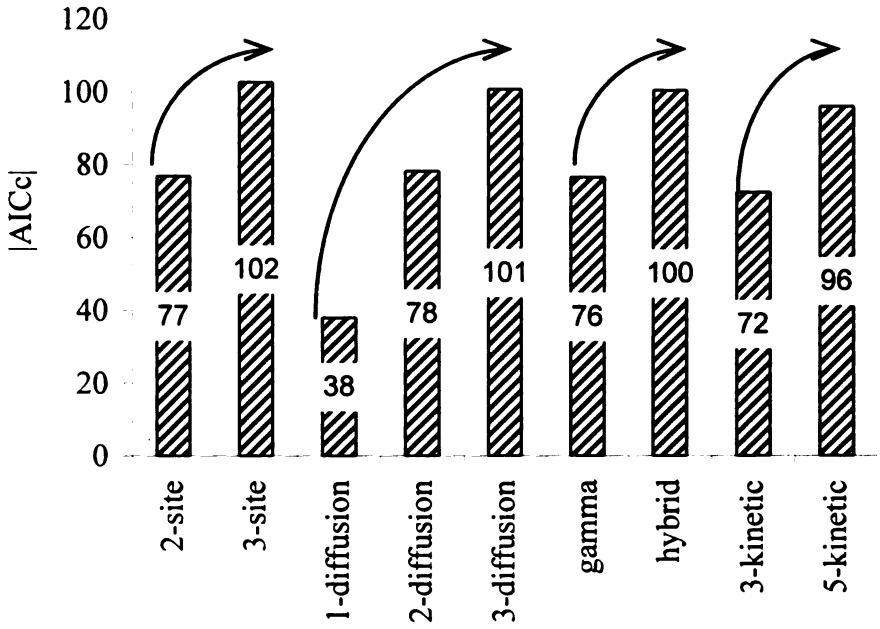

Figure 3-7. Comparison of the AICc for the nine models that were fit to Hartsells-atrazine desorption data.

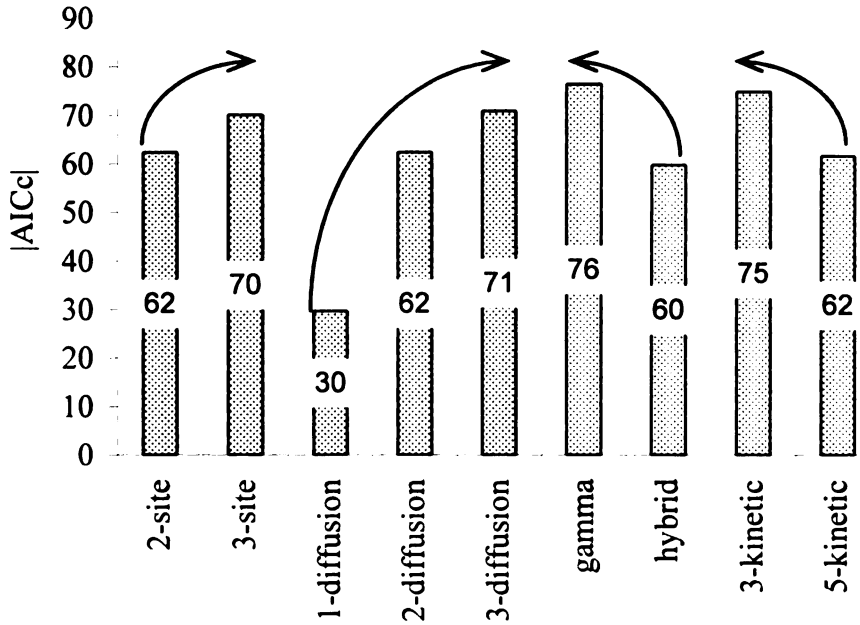

Figure 3-8. Comparison of the AICc for the nine models that were fit to Hartsells-naphthalene desorption data.

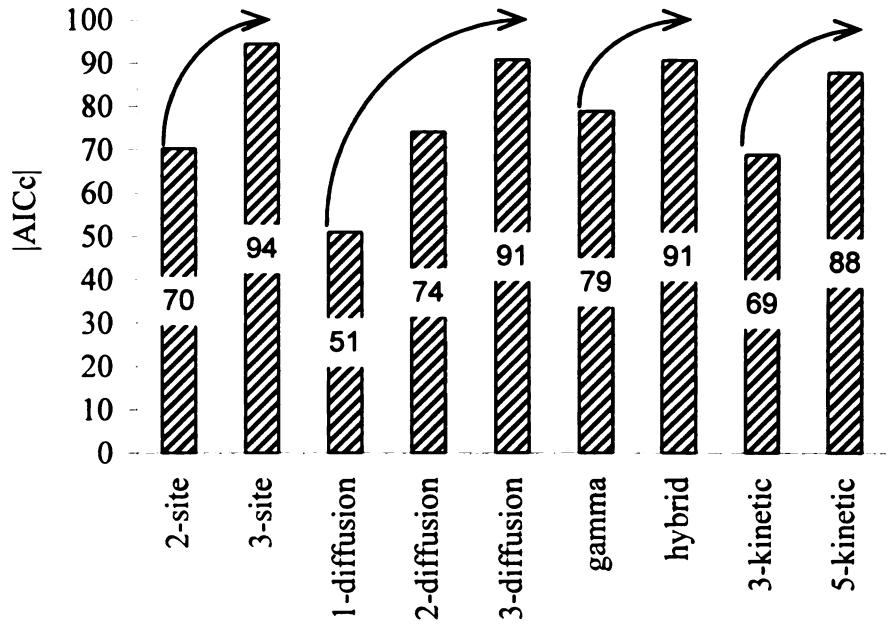

Figure 3-9. Comparison of the AICc for the nine models that were fit to Muck-atrazine desorption data.

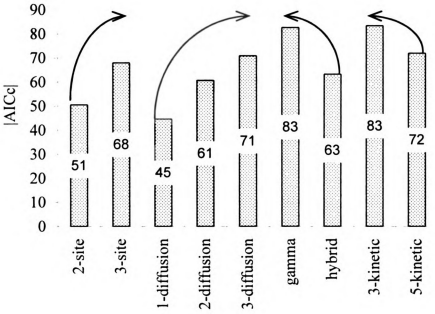

Figure 3-10. Comparison of the AICc for the nine models that were fit to Muck-naphthalene desorption data.

Table 3-1. Selected properties of sorbents used in this study.

Soil	% O.C.[a]	% Sand	% Silt	% Clay	pH	CEC[b] [cmol(+)/kg]
Hartsells	1.29	59.1	32.1	8.78	5.3	7.10
Capac A	3.28	54.6	24.0	21.4	6.8	24.4
Colwood A	7.80	64.2	20.7	15.1	6.0	43.0
Houghton Muck	38.3	ND[c]	ND	ND	5.1	156

[a]O.C.: organic carbon content; [b]CEC: cation exchange capacity; [c]ND: not determined.

Table 3-2. Model equations fit to desorption data sets.

Model Name	Equation	Eq. #	K
Chemical three-site [11, 18, 19]	$\frac{dS_{neq}}{dt} = -k\left(S_{neq} - f_{neq}K_dC\right)$	(3-3)	3
	$S_{nd} = f_{nd}K_dC_{eq(sorp)}$	(3-4)	
Chemical two-site [20-23]	$\frac{dS_{neq}}{dt} = -k\left(S_{neq} - f_{neq}K_dC\right)$	(3-5)	2
Three-parameter pore diffusion	$S_T = S_{eq} + S_{neq} + S_{nd}$	(3-6)	3
	$\frac{\partial S_{neq}}{\partial t} = D\left(\frac{\partial^2 S_{neq}}{\partial r^2} + \frac{2}{r}\frac{\partial S_{neq}}{\partial r}\right)$	(3-7)	
Two-parameter pore diffusion [17]	$S_T = S_{eq} + S_{neq}$	(3-8)	2
	$\frac{\partial S_{neq}}{\partial t} = D\left(\frac{\partial^2 S_{neq}}{\partial r^2} + \frac{2}{r}\frac{\partial S_{neq}}{\partial r}\right)$	(3-9)	
One-parameter pore diffusion [6, 10, 14, 24-26]	$\frac{\partial S}{\partial t} = D\left(\frac{\partial^2 S}{\partial r^2} + \frac{2}{r}\frac{\partial S}{\partial r}\right)$	(3-10)	1
Hybrid gamma/two-site [16]	$\frac{dS}{dt} = \int_0^\infty -k_i\left(S_i - (1-f_{eq})K_dC\right)\frac{k_i^{\alpha-1}\beta^\alpha e^{-\beta k_i}}{\Gamma(\alpha)}dk_i$	(3-11)	3
Gamma distribution [15]	$\frac{dS}{dt} = \int_0^\infty -k_i\left(S_i - K_dC\right)\frac{k_i^{\alpha-1}\beta^\alpha e^{-\beta k_i}}{\Gamma(\alpha)}dk_i$	(3-12)	2
Five-parameter kinetic [7, 9, 17]	$\frac{dS_r}{dt} = -k_rS_r,\ \frac{dS_s}{dt} = -k_sS_s,\ \frac{dS_{vs}}{dt} = -k_{vs}S_{vs}$	(3-13),(3-14) (3-15),(3-16)	4*
	$S_r = f_rS_T,\ S_s = f_sS_T,\ S_{vs} = (1 - f_r - f_s)S_T$	(3-17),(3-18)	
Three-parameter kinetic [8, 9, 27, 28]	$\frac{dS_r}{dt} = -k_rS_r,\ \frac{dS_s}{dt} = -k_sS_s$	(3-19) (3-20)	2*
	$S_r = (1 - f_s)S_T,\ S_s = f_sS_T$	(3-21) (3-22)	

* k_{vs} is set to zero in the five-parameter kinetic model and k_s is set to zero in the three-parameter kinetic model and therefore are not counted as parameters.

Table 3-3. List of Symbols.

AIC	Akaike information criterion
AIC_c	small-sample corrected Akaike information criterion
C	contaminant concentration is the aqueous phase
$C_{eq(sorp)}$	contaminant concentration in the aqueous phase at sorption equilibrium
D	apparent diffusion coefficient
f_{eq}	equilibrium site fraction
f_{nd}	non-desorption site fraction
f_{neq}	Nonequilibrium site fraction
f_r	rapidly desorbing fraction
f_s	slowly desorbing fraction
f_{vs}	very slowly desorbing fraction
K	number of estimated parameters
k	first-order rate coefficient
K_d	soil-water partition coefficient
k_i	first-order rate coefficient for the i^{th} soil compartment
k_r	first-order rate coefficient for the rapid fraction
k_s	first-order rate coefficient for the slow fraction
k_{vs}	first-order rate coefficient for the very slow fraction
n	number of data points
r	radial distance
S	contaminant concentration in soil
S_{eq}	contaminant concentration in the equilibrium soil compartment
S_i	contaminant concentration in the i^{th} soil compartment
S_{nd}	contaminant concentration in the non-desorption soil compartment
S_{neq}	contaminant concentration in the nonequilibrium soil compartment
S_r	contaminant concentration in the rapid compartment
S_s	contaminant concentration in the slow compartment
S_T	total contaminant concentration in all soil compartments
S_{vs}	contaminant concentration in the very slow compartment
t	Time
Γ	gamma distribution function
α	shape parameter
β	scale parameter
$\hat{\sigma}^2$	sample variance

References

1. Kan, A.T., et al., *Irreversible sorption of neutral hydrocarbons to sediments: experimental observations and model predictions.* Environmental Science and Technology, 1998. **32**(7): p. 892-902.

2. Alexander, M., *Aging, bioavailability, and overestimation of risk from environmental pollutants.* Environmental Science and Technology, 2000. **34**(20): p. 4259-4265.

3. Pignatello, J.J. and B. Xing, *Mechanisms of slow sorption of organic chemicals to natural particles.* Environmental Science and Technology, 1998. **30**(1): p. 1-11.

4. Luthy, R., et al., *Sequestration of hydrophobic organic contaminants by geosorbents.* Environmental Science and Technology, 1997. **31**(12): p. 3341-3347.

5. Kukkonen, J., et al., *Sediment characteristics affecting desorption kinetics of select PAH and PCB congeners for seven laboratory spiked sediments.* Environmental Science and Technology, 2003. **37**: p. 4656-4663.

6. Wu, S. and P. Gschwend, *Sorption kinetics of hydrophobic organic compounds to natural sediments and soils.* Environmental Science Technology, 1986. **20**: p. 717-725.

7. Cornelissen, G., et al., *Temperature dependence of slow adsorption and desorption kinetics of organic compounds in sediments.* Environmental Science and Technology, 1997. **31**: p. 454-460.

8. Cornelissen, G., et al., *Rapidly desorbing fractions of PAHs in contaminated sediments as a predictor of the extent of bioremediation.* Environmental Science and Technology, 1998. **32**: p. 966-970.

9. Cornelissen, G., P.C.M. van Noort, and H.A.J. Govers, *Mechanism of slow desorption of organic compounds from sediments: A study using model sorbents.* Environmental Science and Technology, 1998. **32**: p. 3125-3131.

10. Grathwohl, P. and M. Reinhard, *Desorption of trichloroethylene in aquifer material: rate limitations at the grain scale.* Environmental Science and Technology, 1993. **27**: p. 2360-2366.

11. Park, J.-H., X. Zhao, and T. Voice, *Biodegradation of non-desorbable naphthalene in soils.* Environmental Science and Technology, 2001. **35**(13): p. 2734-2740.

12. White, J.C. and M. Alexander, *Reduced biodegradability of desorption-resistant fractions of polycyclic aromatic hydrocarbons in soil and aquifer solids.* Environmental Toxicology and Chemistry, 1996. **15**(11): p. 1973-1978.

13. Brusseau, M.L. and P.S.C. Rao, *Sorption nonideality during organic contaminant transport in porous media.* Critical Reviews in Environmental Control, 1989. **19**(1): p. 33-99.

14. Crank, J., *The Mathematics of Diffusion.* First ed. 1956: Oxford at the Clarendon Press.

15. Connaughton, D.F., et al., *Description of time-varying desorption kinetics: release of naphthalene from contaminated soils.* Environmental Science and Technology, 1993. **27**: p. 2397-2403.

16. Ahn, I.-S., L.W. Lion, and M.L. Shuler, *Validation of a hybrid "two-site gamma" model for naphthalene desorption kinetics.* Environmental Science and Technology, 1999. **33**: p. 3241-3248.

17. Johnson, M., T. Keinath, and W. Weber, *A distributed reactivity model for sorption by sails and sediments. 14. Characterization and modeling of phenanthrene desorption rates.* Environmental Science and Technology, 2001. **35**(8): p. 1688-1695.

18. Park, J.-H., *Bioavailability of sorbed organic contaminants*, in *Department of Civil and Environmental Engineering.* 2000, Michigan State University.

19. Park, J.-H., X. Zhao, and T.C. Voice, *Development of a kinetic basis for bioavailability of sorbed naphthalene in soil slurries.* Water Research, 2002. **36**: p. 1620-1628.

20. Rao, P.S.C., J.M. Davidson, and H.M. Selim, *Evaluation of conceptual models for describing nonequilibrium adsorption-desorption of pesticides during steady-flow in soils.* Soil Science Society of Americal Journal, 1979. **43**: p. 22-28.

21. Selim, H.M., J.M. Davidson, and P.S.C. Rao, *Transport of reactive solutes through multilayered soils.* Soil Science Society of Americal Journal, 1977. **41**: p. 3-10.

22. van Genuchten, M.T., *Two-Site/Two-Region Models for Pesticide Transport and Degradation: Theoretical Development and Analytical Solutions.* Soil Science Society of Americal Journal, 1989. **53**(5): p. 1303-1310.

23. Cameron, D.R. and A. Klute, *Convective-dispersive solute transport with a combined equilibrium and kinetic adsorption model.* Water Resources Research, 1977. **13**(1): p. 183-188.

24. Farrel, J. and M. Reinhard, *Desorption of halogenated organics from model solids, sediments, and soils under unsaturated conditions. 2. Kinetics.* Environ. Sci. Technol., 1994. **28**: p. 63-72.

25. Werth, C.J. and M. Reinhard, *Effects of temperature on trichloroethylene desorption from silica gel and natural sediments. 2. kinetics.* Environmental Science and Technology, 1997. **31**: p. 697-703.

26. Harmon, T.C. and P.V. Roberts, *Comparison of intraparticle sorption and desorption rates for a halogenated alkene in a sandy aquifer material.* Environmental Science and Technology, 1994. **28**: p. 1650-1660.

27. Johnson, M.D. and J. Weber, W.J., *Rapid prediction of long-term rates of contaminant desorption from soils and sediments.* Environmental Science and Technology, 2001. **35**: p. 427-433.

28. Karickhoff, S.W. and K.R. Morris, *Sorption dynamics of hydrophobic pollutants in sediment suspensions.* Environmental Toxicology and Chemistry, 1985. **4**: p. 469-479.

29. Englezos, P. and N. Kalogerakis, *Applied Parameter Estimation for Chemical Engineers*. Chemical Industries, ed. H. Heinemann. 2001, New York: Marcel Dekker, Inc.

30. Burnham, K.P. and D.R. Anderson, *Model Selection and Inference*. First ed. 1998, New York City: Springer-Verlag.

31. Ginzburg, L.R. and C.S.J. Jensen, *Rules of thumb for judging ecological theories.* Trends in Ecology and Evolution, 2004. **19**(3): p. 121-126.

Chapter 4. Enhanced removal of naphthalene by two plant species used for phytoremediation

Abstract

The enhanced removal of naphthalene from soil by a monocot, big bluestem (*Andropogon gerardii*), and a dicot, white mulberry (*Morus alba*), has been demonstrated over a period of 186 days using two different soils. Soil naphthalene concentrations determined by solvent extraction were lower for the planted treatments than in the unplanted treatments at the end of the trial. The amount of naphthalene that is water extractable approaches a constant value for both unplanted treatments. This implies that a fraction of naphthalene that is water extractable is not available for gaseous diffusion. However, the water extractable portion of naphthalene continues to decrease in all planted treatments. This result is significant as a fraction of naphthalene that is not mobile by gaseous diffusion is available to the plant's transpiration stream.

Introduction

Phytoremediation is an emerging and promising technique for the cleanup of organic contaminants[1-5]. It has widely been perceived as a low-cost alternative to other remediation technologies[6-10]. However, phytoremediation may be subject to the same bioavailability constraints as other bioremediative technologies, e.g. microbial biodegradation[11-17]. In microbial bioremediation, bioavailability can be limited by the extent and rate of desorption from the soil matrix to the microorganism[17], meaning that mass transfer is a critical factor in most cases of bioremediation[12]. Similarly, desorption may limit the bioavailability of organic contaminants for phytoremediation. Low bioavailability limits the endpoint contaminant concentration achievable by microbial bioremediation, and could limit the rate and degree of phytoremediation. Because regulatory agencies can set endpoint contaminant criteria at soil concentrations that are below the amount that is able to desorb, often a significant fraction of contaminant is difficult—but necessary—to remove. As such, a demonstrated ability to achieve the low-level endpoint criteria set by regulatory agencies would enhance phytoremediation's appeal.

Several studies have demonstrated the efficacy of plants for removing PAHs (polyaromatic hydrocarbons) from soil. Aprill and Sims[18] showed that eight varieties of prairie grass were found to enhance the removal of benzo(a)anthracene, chrysene, benzo(a)pyrene and dibenzo(a,h)anthracene. Naphthalene removal from a field plot was enhanced by the addition of prairie buffalo grass (*Buchloe dactyloides* var. *prairie*)[19]. Alfalfa (*Medicago sativa* L.), switchgrass (*Panicum vergatum*) and little bluestem (*Schizachyrium scoparius*) removed 56, 57 and 47 percent, respectively, of the total

PAHs at a manufactured gas plant[20]. The presence of tall fescue (*Festuca arundinacea*) enhanced the degradation of benzo(a)pyrene in soil[21]. A growth chamber study using tall fescue and switchgrass degraded more pyrene than an unplanted control[22]. The rhizosphere soils of tall fescue and wheat (*Triticum aestivum*) contained a greater amount of phenanthrene and pyrene than did an unplanted treatment[23], demonstrating enhanced PAH mobility. Alfalfa and reed (*Phragmites australis*) were shown to degrade 74.5 and 68.7 percent, respectively, of the 16 EPA priority pollutant PAHs in two years[24]. Pyrene degradation was greater in planted versus unplanted treatments[25] and levels of pyrene declined from 100 ppm to 2.4 ppm in 24 weeks. A number of studies have demonstrated the ability of plants to remove PAHs from soil, though incomplete removal is a common result in many of these trials.

The final achievable contaminant level is often limited by the PAH bioavailability. Low bioavailability can be attributed to slow desorption from the soil matrix. Several studies have demonstrated the limitations of hydrophobic organic contaminant desorption. The effort presented in Chapter 3 of this dissertation demonstrated the tendency of organic contaminant desorption to be segregated into different behavioral regimes, i.e. equilibrium, nonequilibrium, and non-desorption. The non-desorption regime is characterized by very slow desorption (i.e. immeasurably slow) from the soil matrix. It has been hypothesized that contaminant sorbed to non-desorption regimes is not bioavailable. However, the concept of bioavailability is somewhat more complex, as microbial degradation rates tend to be faster than expected and non-desorbable material can be degraded. White and Alexander[26] found that phenanthrene and naphthalene sorbed to desorption-resistant soil fractions were biodegraded, albeit slowly. Guerin and

Boyd demonstrated that *Pseudomonas putida* 17484 accessed naphthalene sorbed to domains deemed unavailable for biodegradation, a result attributed to cell attachment[27]. Evidence supporting enhanced bioavailability by attachment has been gathered by Park et al.[16, 28, 29] with *Pseudomonas putida* G7 and NCIB 9816-4. Enhanced liquid-phase biodegradation rates were observed and attributed to solid-phase degradation. Park et al. determined that naphthalene and atrazine[30] sorbed to non-desorbable regimes could be degraded by microorganisms. A further study involving soil-sorbed biphenyl demonstrated biodegradation by attached gram-positive and a gram-negative bacteria[15]. Organisms in close proximity with the sorbed contaminant, as is the case with cell attachment, appear capable of enhancing bioavailability. Likewise, the contact that exists between the plant root and the soil matrix may also enhance bioavailability.

The focus of this investigation is on understanding the relationship between the contaminant removed in planted systems and the desorbability of the remaining contaminant. White mulberry (*Morus alba*) and big bluestem (*Andropogon gerardii*) were grown in two soils for assessing the removal of soil-sorbed naphthalene and inferring the mechanisms responsible for limiting this removal. Desorption is thought to be the first step, and a limiting step, in the phytoremediation of sorbed organic contaminants. Contaminant desorption is followed by transport in the aqueous phase to the root surface, where the contaminant can be taken into the root with the transpiration stream water. This description implies that desorption limits the contaminant bioavailability, and hence, the degree of phytoremediation. However, analogous to microbial bioavailability, the existence of mechanisms responsible for enhancing bioavailability would greatly add to phytoremediation's appeal as a cleanup technology.

Plants are associated with a variety of mechanisms that may be able to remove contaminants residing in non-desorption domains of soil. The secretion of enzymes[9, 31], such as monooxygenases and peroxidases, may degrade recalcitrant contaminants. Secretion and exudation of compounds that stimulate the microbial consortia to degrade contaminants is also a potential mechanism for enhancing desorption [9], as is the plant promoted production of surfactants[9]. Any combination of these mechanisms may be manifested as an enhancement of PAH bioavailability. The presence or absence of this bioavailability enhancement effect will alter the application of plants for remediation of contaminated soils. A plant's tendency to enhance bioavailability, analogous to a microbe's tendency to enhance bioavailability, is important knowledge when applying phytoremediation as a cleanup option and achieving the necessary regulatory endpoints.

Materials and Methods

Soil contamination

Two soils, Spinks A horizon (SpAf) and Kalkaska A horizon (Kal A), were sterilized by exposure to 5 Mrads of gamma radiation at the Phoenix Memorial Laboratory (University of Michigan, Ann Arbor, MI). The sterile soil was placed in a one gallon steel can that was sterilized in an autoclave. 100 ml of a 1:1 mixture of acetone:pentane was used as the carrier solvent for delivering 500 mg of naphthalene to 1 kg of soil. Naphthalene was added to air dry SpAf and Kal A soils to achieve a concentration of 500 ppm. The soil filled cans were mixed by rotation at approximately 12 rpm for 12 hours. Table 1 contains the measured soil characteristics for SpAf and Kal A.

Plant tissue culture

Two species of plant were used for this experiment, *Andropogon gerardii* and *Morus alba*. *A. gerardii* is a monocot with a fibrous root system and *M. alba* is a dicot. *A. gerardii* seeds were germinated on moist, sterile filter paper placed in a Petri dish. The Petri dishes were placed in a growth chamber set for a 16 hour to 8 hour light to dark cycle and a temperature of 26°C. *M. alba* was propagated by vegetative stem cuttings from a single plant that was surface sterilized with a ten percent bleach solution. Nodal explants were placed in shooting media for two weeks and then moved to rooting media for an additional three weeks. Plants that were approximately two centimeters tall were transplanted to soil.

Planted bioreactor treatments

Plants were placed in contaminated soil using aseptic technique in a laminar flow hood. For the unplanted treatments, ten milliliter test tubes were filled with 10 grams of sterile, contaminated soil. About six grams of soil were poured into the test tubes to be used for the planted treatments, then the plant was placed in the tube and the remainder (about four grams) of the soil was poured over the roots. Two milliliters of one-half strength MS (Murashige and Skoog) media were added to each test tube. The test tubes were placed in sterile, coupled, sand-filled Magenta boxes (Figure 4-1). Four test tubes, each with one plant were placed in the coupled Magenta GA7 boxes. Bioreactor assemblies were placed in a plant growth chamber set at a 16 hour to 8 hour light to dark cycle and a temperature of 28°C. Sterile water was added to the sand to maintain high humidity within the Magenta box. Plants were watered as needed throughout the course of the experiment. Initially, two milliliters of water was added to each tube. Planted treatments were watered again approximately two weeks later as the transpiration by the plant became significant. Thereafter, plants were watered with 1/2X MS as needed. Each watering event proceeded in a laminar flow hood using sterile technique. A needle, attached to the syringe, was used to puncture a septum on top of each coupled box, allowing for each planted replicate to be watered. The humidity in the Magenta box served to slow the water loss from the soil environment by transpiration.

Sampling

The Magenta boxes were harvested at five different time points in a laminar flow hood. The plant was removed from the soil using forceps and a metal spatula. The roots were cut from the shoots and washed in purified water. Soil from the test tube was

subdivided into samples for solvent extraction, sequential water extraction, moisture content, and sterility. Solvent extractions were performed placing approximately one gram of soil in a glass 4 ml vial with a PTFE (Teflon) liner. The vials were filled to the top (no head space) with methanol. The contents of the vials were mixed via rotation at 12 rpm for 3 days. After mixing, the vials were centrifuged for 5 minutes using a benchtop centrifuge, and the supernatant was sampled for subsequent analysis. Sequential water extractions were performed by placing approximately 1.5 grams of soil in a 4 ml glass vial with a PTFE liner. The vials were filled to the top with 1/2X MS (Murashige and Skoog media). The contents of the vials were mixed via rotation at 12 rpm for 3 days. The samples were centrifuged and the supernatant was collected for subsequent analysis. Fresh 1/2X MS was added to the vial with the previously water extracted soil, a process that is reiterated until naphthalene is not detected in the supernatant. Both the solvent extraction and the water extraction samples were analyzed by HPLC (10 μm, C18 column) using UV and fluorescence detection. Water content was measured gravimetrically by first placing one to ten grams of soil in an aluminum weighing pan and then placing them in a convection oven overnight at 110°C. Sterility was checked by placing approximately 0.1 gram of soil in a sterile Eppendorf tube and adding one milliliter of cell extraction buffer (contains EGTA and Tween 20). The tubes were placed on a laboratory shaker set at 120 rpm for ten minutes. One hundred μl of the slurry was sampled and spread on a Petri plate containing YEPG media (yeast extract, polypeptone and glucose). If any colonies appeared, the plate was subjected to the indole assay (a small amount of solid indole is added to the lid of the plate causing colonies that express naphthalene dioxygenase to turn blue as indole is converted to indigo). Root

tissue was analyzed using the WinRhizo image analysis software. This software package allows for measurement of root surface area, volume, and color. Subsequently, the roots and shoots were dried and weighed to determine dry weight.

Mathematics

The mathematical model used to describe the data was formulated by performing an overall mass balance on naphthalene, a mass balance on a nonequilibrium site fraction, and a mass balance on an immobile-water site fraction. Figure 4-2 is a depiction of the soil as described by the model equations formulated for this study and Figure 4-3 is a box diagram of this model. The model equations for the unplanted treatments are presented in equations 4-1 through 4-3.

$$V_w \frac{\partial C_w}{\partial t} + m_s \frac{\partial S_{eq}^m}{\partial t} + m_s \frac{\partial S_{neq}^m}{\partial t} + m_s \frac{\partial S_{eq}^{im}}{\partial t} + V_g \frac{\partial C_g}{\partial t} = D_g V_g \frac{\partial^2 C_g}{\partial z^2} \qquad \text{Equation (4-1)}$$

$$\frac{\partial S_{neq}^m}{\partial t} = -k_{neq}\left(S_{neq}^m - K_d f_{neq} C_w\right) \qquad \text{Equation (4-2)}$$

$$\frac{\partial S_{eq}^{im}}{\partial t} = 0 \qquad \text{Equation (4-3)}$$

V_w is the volume of soil solution in the test tube and C_w is the concentration of naphthalene in the soil solution. The mass of soil is given the symbol m_s and the soil

itself is divided into three site fractions. S_{eq}^{m} is the concentration of naphthalene in the soil solid that is connected and in equilibrium with the mobile soil solution, where mobility is defined as contaminant that can be transported in the gas phase. S_{eq}^{im} is the concentration of naphthalene in the soil solid that is in equilibrium with the immobile soil solution (i.e. contaminant that cannot be transported in the gas phase). S_{neq}^{m} is the concentration of naphthalene that is not in equilibrium with the mobile soil solution. The three soil concentrations sum to equal the total soil concentration. V_g is the volume of soil gas and C_g is the concentration of naphthalene that is present in the soil gas. D_g is the diffusivity of naphthalene in air. The parameter k_{neq} is the first-order desorption rate coefficient for the nonequilibrium domain. The parameters f_{eq} and f_{neq} are the site fractions for the mobile-equilibrium domain and the mobile-nonequilibrium, respectively. The variable t is time and z is the vertical dimension.

Naphthalene is assumed to exit the soil by gaseous diffusion only. Transport of naphthalene is dynamically limited by desorption from the nonequilibrium site fraction. The extent of naphthalene removal from the soil is limited by the amount sorbed to soil domains in equilibrium with immobile water. This fraction is not in contact with the mobile soil air and therefore does not diffuse out of the soil. However, the immobile domain is water extractable, whereas the nonequilibrium domain is not measurably extracted with water. All of the soil domains are assumed to be extractable with methanol. The model parameters (i.e. f_{eq}, f_{neq}, and k_{neq}) were estimated assuming that the naphthalene loss from the unplanted soils was solely attributed to gaseous diffusion.

The model formulation for the planted treatments is modified to contain an added term describing the uptake of contaminant by the transpiration stream. Figure 4-4 is a depiction of the rhizosphere soil as described by the model equations formulated for this study and Figure 4-5 is a box diagram of this model. The model is presented in equations 4-4 through 4-6.

$$V_w \frac{\partial C_w}{\partial t} + m_s \frac{\partial S_{eq}^m}{\partial t} + m_s \frac{\partial S_{neq}^m}{\partial t} + m_s \frac{\partial S_{eq}^{im}}{\partial t} + V_g \frac{\partial C_g}{\partial t} = D_g V_g \frac{\partial^2 C_g}{\partial z^2} - k_p V_w C_w$$

Equation (4-4)

$$\frac{\partial S_{neq}^m}{\partial t} = -k_{neq}\left(S_{neq}^m - K_d f_{neq} C_w\right)$$

Equation (4-5)

$$\frac{\partial S_{eq}^{im}}{\partial t} = -\frac{k_p V_w}{m_s K_d + V_w} S_{eq}^{im}$$

Equation (4-6)

An additional first-order mechanism is used to describe the effect that plant roots have on the mass of naphthalene in the soil. The additional first-order mechanism is parameterized by k_p, the first-order naphthalene removal coefficient.

The added mechanism is assumed to act on both equilibrium domains, as large roots grow in the soil macropores (assumed to comprise the mobile region) and root hairs are likely able to access water in the soil micropores (i.e. the immobile region). Plants are not assumed to enhance the rate at which contaminant desorbs from the nonequilibrium domain. The parameter k_p is a lumped parameter with contributions from

the plant root density, the plant transpiration stream concentration factor and the average daily water uptake rate.

Parameter estimation was accomplished using the Gauss-Newton method for coupled-partial differential equations. The state variables that were fit are the methanol extractable naphthalene mass and the sequential water extractable naphthalene mass. The adjustable parameters are: f_{eq}, f_{neq}, and k_{neq} for the unplanted treatments, and k_p for the planted treatments. The accepted tolerance for the convergence criterion was assumed to be equal to 10^{-3}. All model equations and the partial differential equations for the sensitivity coefficients were solved using the finite element method. After the equations were cast in semi-discrete form, a finite difference time-stepping scheme was used to generate model profiles for each state variable.

Results and Discussion

Description of data

The data is plotted along with the model fits in Figure 4-6. For the unplanted treatments, the data collected from the methanol extractions and the sequential water extractions are observed to generate two distinct profiles. The profiles for the unplanted treatments appear to change rapidly at short times, before approaching a limiting value at long times. At short to intermediate times, a significant deviation exists between the methanol and water extraction data. A fraction of material that was methanol extractable was not water extractable. At later times, both the methanol and water extraction data sets appear to converge to nearly the same value. This mass is larger than zero, and does not appear to approach zero at an appreciable rate.

Similar profiles exist for the planted treatments, though the final converged value is lower than the unplanted treatments. Plant growth, as shown in plots of the root surface area in Figures 4-7 and 4-8, correlates with the enhanced removal of naphthalene from the test soils.

Discussion of the data collected for the unplanted treatments

As seen in the plots of the unplanted treatments present in Figure 4-6, both the methanol and water extraction data can be divided into two distinct regimes—each regime characterized by a different rate of naphthalene loss. In both data sets, the first regime is characterized by a much faster loss rate than is the loss rate in the second regime. Possible mechanisms for the loss of naphthalene from the unplanted test tube soils are: volatilization[32, 33], biodegradation[34-37] and binding to non-extractable domains[38-41]. Because of the rate of loss in the first regime, volatilization is the

suspected mechanism. The loss of naphthalene during the first 20 days, as seen in Figure 4-6, occurs at a rate that can be parameterized by the gaseous diffusivity for naphthalene in the soil atmosphere, a value traditionally estimated using the Millington-Quirk formulation[42]. This suggests that naphthalene loss can be attributed to volatilization, not biodegradation or binding to non-extractable domains of soil. Furthermore, γ-irradiation was used to sterilize all soils—for the purpose of minimizing the biodegradation potential in the soil. To determine the extent of any microbial contamination, all soils were plated at each sampling event, as the release of microbial endophytes into the soil was anticipated[43-46]. Each plate was also subjected to the indole assay to test for naphthalene dioxygenase activity. Direct plate counts for the unplanted treatments always resulted in less than 10^3 CFU per gram of soil. The absence of indole positive colonies—an indole positive colony is a colony that is actively converting indole to indigo—is consistent with no expression of the naphthalene dioxygenase enzyme. Though bacteria are present, they are not actively expressing this enzyme. Naphthalene may also bind to soil constituents to form non-extractable residues[47]. The formation of these residues was not observed in previous studies using either of these test soils[48]. From a toxicological perspective, naphthalene that forms a non-extractable residue may not be a risk to human health[11].

The two regimes that Figure 4-6 can be divided to are characterized by a rapid initial loss of naphthalene that is followed by a much slower rate of loss—an observation supported by published literature[33, 49]. The decreased loss rate in the second regime can be characterized by slow mass transfer from the soil matrix[50-55]. In a previous study, both soil types have demonstrated significant mass transfer limitations in batch soil

studies[28, 29, 48, 56], so biphasic behavior was expected in this study. A difference exists between the methanol extractable and water extractable component of the sorbed naphthalene. This difference is likely due to naphthalene sorbed to a hydrophobic component of the soil in which desorption to the soil solution is kinetically limited[55, 57-61]. This regime of the soil is responsible for the slow loss of naphthalene observed in the methanol extraction profile. Though desorption from this regime can be witnessed over the experimental time-course of 186 days, significant desorption was not witnessed over the water extraction time-course of 3 days. However, much of the naphthalene remaining in the soil after 186 days remains water extractable, as seen in Figure 4-6. Several explanations exist for the water extractability of naphthalene at long times. The simplest explanation is that naphthalene is released from aggregate micropores after the abrasion of the aggregate that occurs during successive water extractions. Naphthalene, residing in domains that are not in equilibrium with the soil gas, is released upon breaking the aggregate by mixing, but this naphthalene is not released during the course of the experiment. Further possibilities for this behavior exist, as perhaps naphthalene is retained in micropores that have been blocked by precipitated inorganic materials[62]. This entrapment of naphthalene is expected to hinder volatilization, but the naphthalene would likely be water extractable as the precipitate dissolves. Another explanation for restricted naphthalene volatilization is the slow desorption through water that is arranged in a highly organized. Water has been found to behave in this manner in the soil micropores that contain hydrophobic regions[63]. Regardless of the manner in which naphthalene is retained in micropores, contaminant in these domains of soil may not be in equilibrium with the soil gas, i.e. a fraction of the total naphthalene is not governed by

Henry's law. Again, regardless of the retaining mechanism, the explanation for the significant pool of water extractable naphthalene resides in the manner in which the water extractions were conducted—namely by mixing the soil slurry and sequentially decanting and re-adding fresh solution. Mixing of the slurry may have resulted in a disaggregation of the soil structure, a dissolution of precipitated material, or a disruption of the micropore solution, all of which lead to naphthalene desorption into the bulk solution. Transfer from this region under the experimental conditions is likely unmeasurable when compared to transfer from the other limiting regimes present in the soil. Though transfer from this regime is too slow to measure in the test tubes soils, the material contained in this regime remains water extractable.

Discussion of data collected for planted treatments

Both planted soils contained decreased concentrations at long times when compared to the unplanted treatments, as seen by comparing the treatments in Figure 4-6. Clearly, the addition of plants facilitates an increase in naphthalene loss from the test tube soil. In addition to a removal mechanism attributed to the plant, the mechanisms responsible for naphthalene removal in unplanted soils are likely occurring. Volatilization remains a mechanism for contaminant removal throughout the run time for planted and unplanted treatments alike. Transpiration is likely responsible for further naphthalene removal[64]. Mechanistically, naphthalene in the soil solution can be taken into the plant through the transpiration stream and removed from the soil[64]. A decreased water extractable mass, when compared to the unplanted treatments, suggests that the transpiration stream is accessing naphthalene associated with the soil micropores. Naphthalene residing in both macro- and micropores can enter the transpiration stream as

plants are capable of transpiring water from both macro- and micropores non-preferentially[65]. Removal of water from these regimes by the roots can also promote increased volatilization as micropore water is no longer restricting the access of soil gas. The combined effect of increased volatilization and transpiration amounts to the increased loss observed in the planted treatments. Thus plants are likely able to enhance desorption from regions which are not in equilibrium with the soil gas, and in so doing, increase the rate of mass transfer from the soil.

Model formulation for the unplanted treatments

Examination of the collected data with an equilibrium model fails to predict the deviation that exists between the methanol extraction and water extraction data sets, as shown in Figure 4-9. Though the initial loss rate of naphthalene is consistent with the volatilization component of an equilibrium model—i.e. a model that uses Henry's partitioning and Fickian diffusion in the gas phase—the intermediate and late rates of loss are not predictable by an equilibrium formulation alone. Also, the amount of material that is extractable by sequential water extraction is not accurately predicted. A deviation exists between the methanol and water extraction data sets. The magnitude of this deviation can be described by a mass transfer expression. This mechanism states that a fraction of contaminant that is available for volatilization, albeit slowly, is not appreciably water extractable. Essentially, there is a longer time period for contaminant loss by volatilization than is the time period used for the sequential water extractions. The addition of a mass transfer mechanism accounts for the difference observed between the methanol and water extractable fractions as depicted in Figure 4-10. Though the

methanol extraction data is adequately modeled, the water extraction data significantly deviates from the model fit at intermediate and long times. An additional mechanism is needed to account for naphthalene that is resistant to volatilization, though water extractable—as the methanol and water extraction data sets converge to nearly the same value at the 186 days. Water in immobile regions of soil, such as the aggregate micropores, may retain naphthalene that is not in equilibrium with the soil gas. This material is considered to be water extractable throughout the experimental time course, but not volatile. The best-fit lines, presented with the data in Figures 4-6 and 4-9, are generated using the three-regime model. This model was formulated using an equilibrium regime, a mass transfer limited regime, and an immobile regime. This model accurately fits the acquired data as the coefficient of determination is 87 and 88 percent for the SpAf and KalA soils respectively.

Model formulation for the planted soil

Plants were observed to decrease the amount of naphthalene that remained in the soil at the end of the experiment. The loss of naphthalene from the planted treatments is consistent with the removal of microporous water via transpiration, a phenomena that has been demonstrated previously[65]. An additional mechanism is needed to account for this enhanced removal, and was done so assuming first-order kinetics. The model fits presented in Figure 4-6 include best-fit lines that were generated using the three regime model with the addition of a first-order removal mechanism attributed to the plant. The values of the coefficients of determination range from 90 to 92 percent, and thus the data

are accurately described. Material that is associated with immobile domains, and not in equilibrium with the soil gas, may be removed by phytoremediation.

Discussion of parameters

Table 4-2 includes the parameters that were fit for both unplanted treatments using the Gauss-Newton method. The equilibrium regime was larger in the SpAf soil than in the Kal A soil as the value for f_{eq}^{m} is larger for SpAf than for the Kal A soil. The nonequilibrium regimes were of comparable size in both treatments, while the size of the immobile regime was larger in the Kal A soil. This implies that a greater amount of naphthalene will be present in the micropores of Kal A soil than in SpAf soil. The desorption rate coefficient, k_{neq}^{m}, is larger in the Kal A soil than in the SpAf soil, though this difference is not significant. Interestingly, the value of k_p does not depend upon the species of plant as much as the soil type.

Conclusion

These results are significant as evidence that plants are able to enhance the removal of contaminants from soil by transpiring water containing naphthalene in micropores. The conceptual model that results from the analysis of unplanted soil is presented in Figure 4-3. Mass transfer of naphthalene in soil is thought to occur by a number of mechanisms, including: 1) instantaneous mass transfer due to equilibrium partitioning between the soil solid and the soil solution, 2) rate limited transfer from the soil solid to the soil solution, and 3) Henry's partitioning from the soil solution into the soil gas followed by gaseous diffusion through the air-filled void spaces. Naphthalene

residing in the micropores of the soil aggregates is not included as a transfer process, as this material is not in equilibrium with the soil gas. Conversely, the depiction of the planted system, as shown in Figure 4-5, depicts the ability of the plant to access naphthalene in aggregate micropores. The authors speculate that this removal is due to converting the immobile water in the aggregate pores to mobile (i.e. advective) water. This process would result in transporting the naphthalene to the macroporous soil solution, where the processes of volatilization or plant uptake could remove the naphthalene from the test soil. The conceptual model, formulated by interpreting the data gathered from methanol and sequential water extractions, justifies the use of plants for removing contaminants that may reside in microporous regimes of soil. Finally, the results of this study further advocate the selection of plants as a remediation technology, as the extent and rate of removal are enhanced in planted systems.

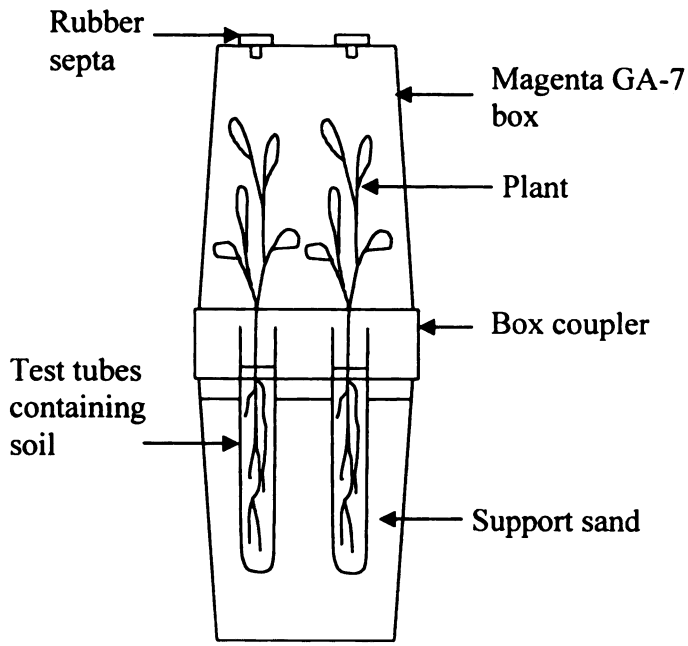

Figure 4-1. The planted bioreactor.

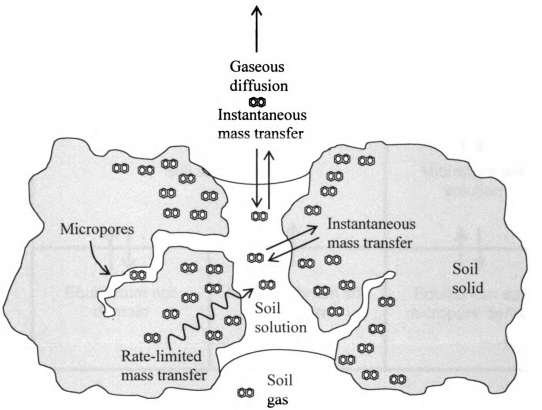

Figure 4-2. The conceptual description of naphthalene transport in unplanted soil that was developed upon interpretation of the methanol and water extraction data.

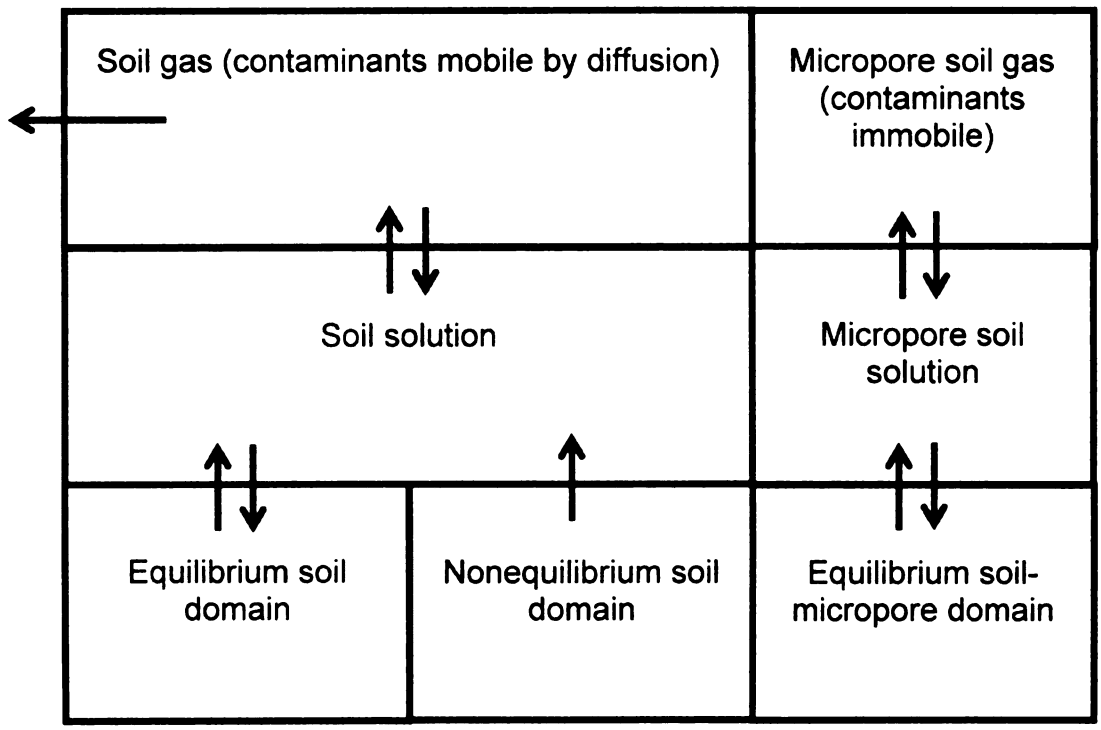

Figure 4-3. Box model for the unplanted treatments.

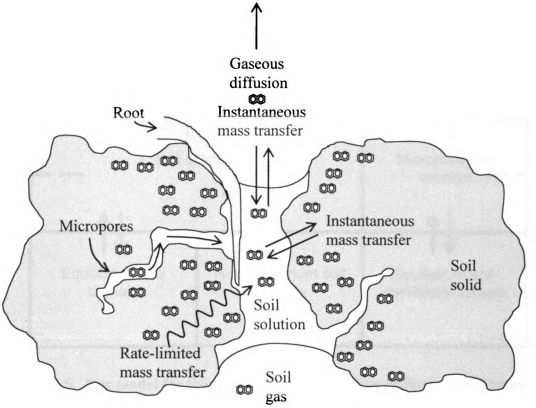

Figure 4-4. The conceptual description of naphthalene fate and transport in planted soil that was developed upon interpretation of the methanol and water extraction data.

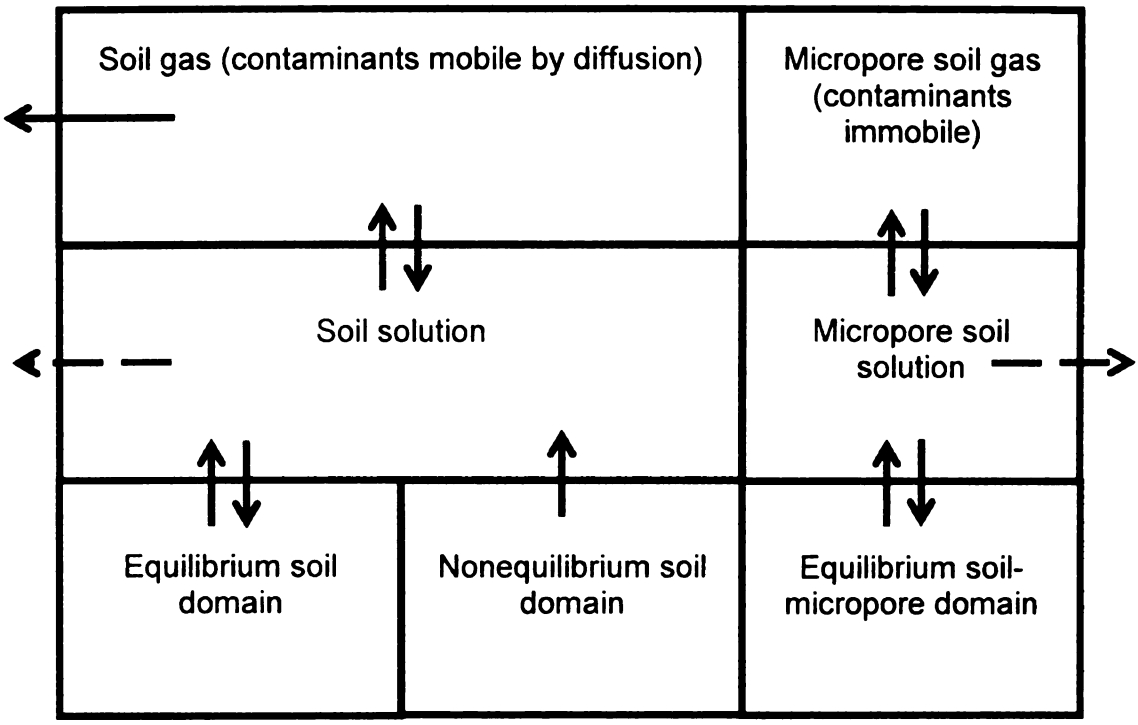

Figure 4-5. Box model for the planted treatments. The dashed arrows represent naphthalene transport that is attributed to the transpiration stream.

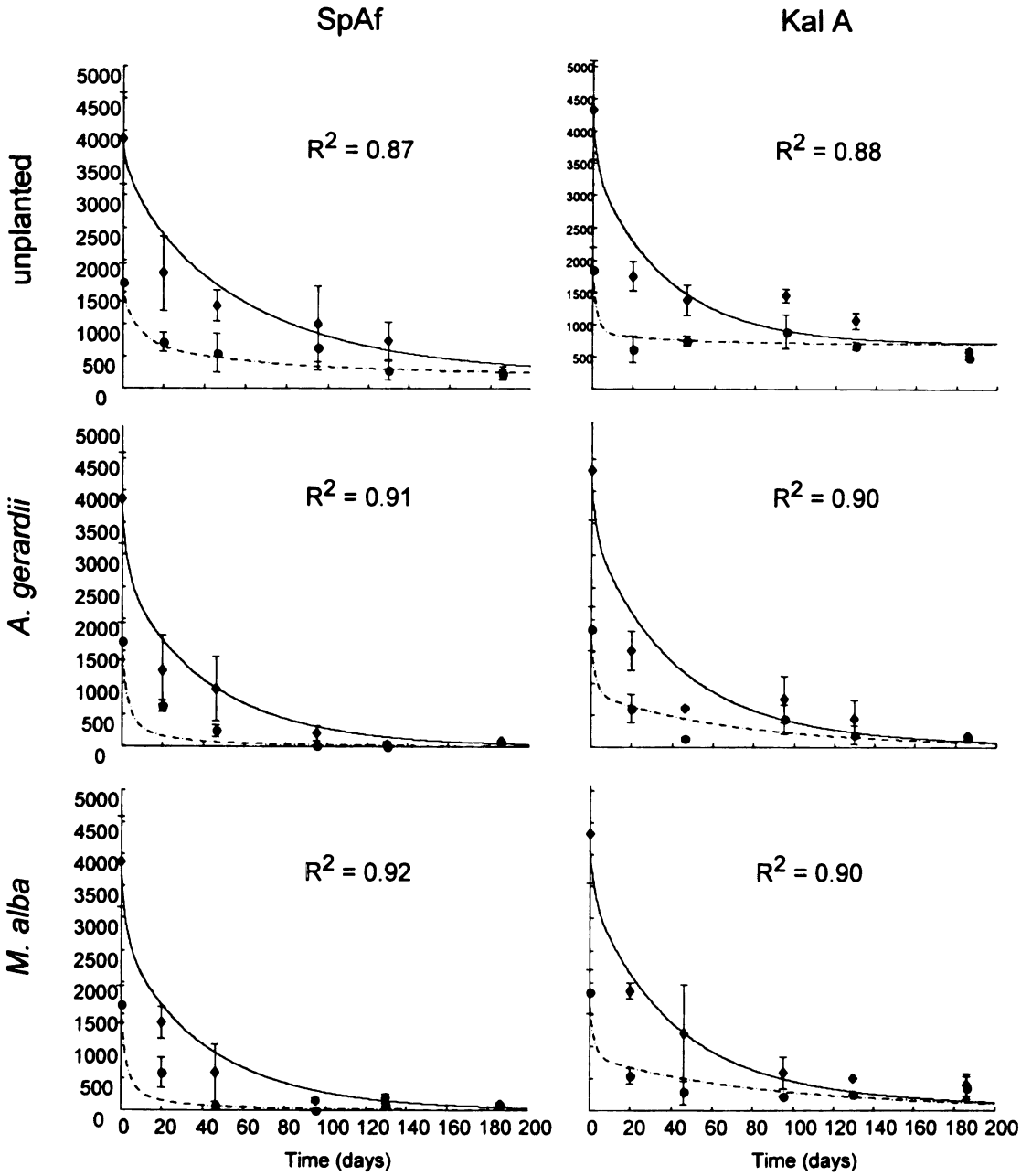

Figure 4-6. Plots of methanol extraction data, water extraction data, and models fits for the six treatments. The Y-axis is the naphthalene mass in µg. The diamonds are the methanol extraction data points and the circles are the water extraction data points. The solid line is the methanol extraction best-fit line and the dashed line is the water extraction best-fit line.

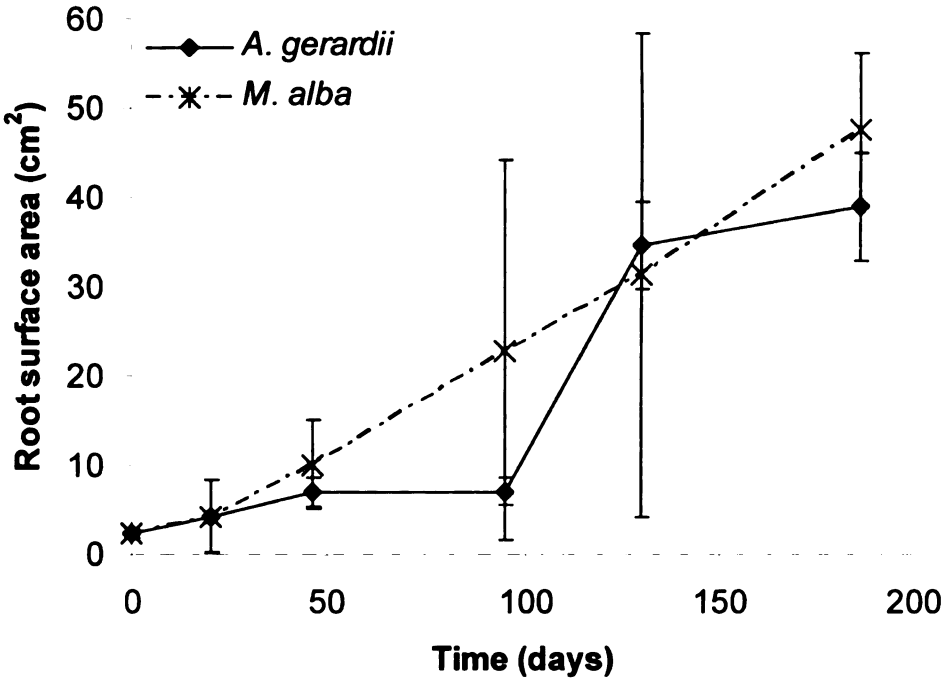

Figure 4-7. Root surface area profile for *A. gerardii* and *M. alba* in SpAf soil.

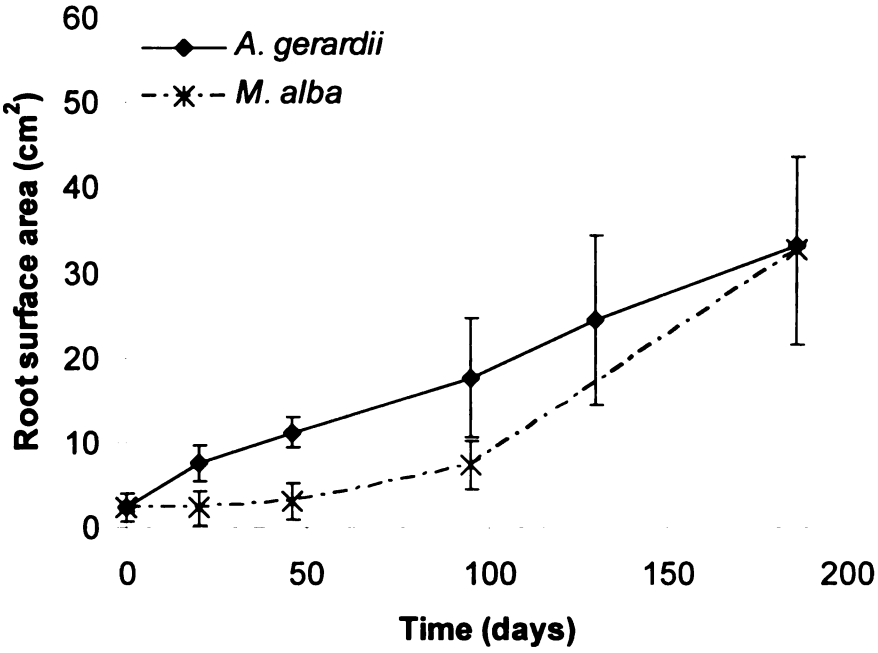

Figure 4-8. Root surface area profile for *A. gerardii* and *M. alba* in Kal A soil.

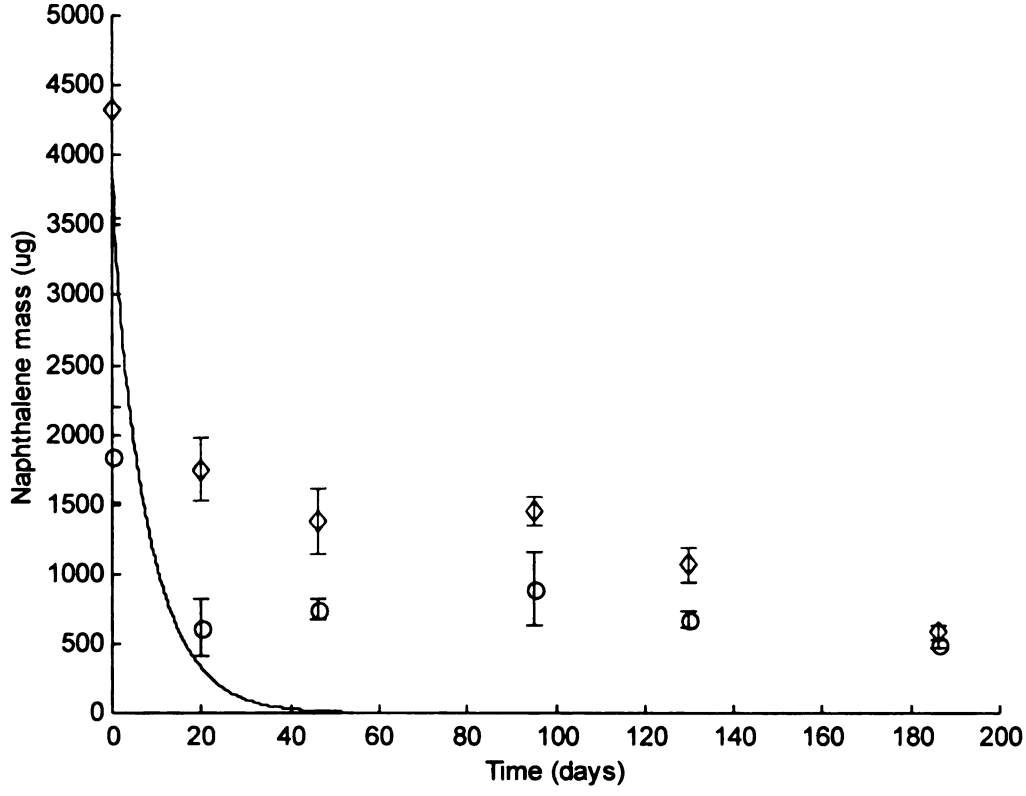

Figure 4-9. Plot of methanol extractable naphthalene mass and water extractable naphthalene mass versus time for Kal A soil that is unplanted. The diamonds (♦) are the methanol extraction data and the circles (○) are the water extraction data. Standard deviation error bars are included on each point. The solid line is the model fit of the methanol and water extraction data.

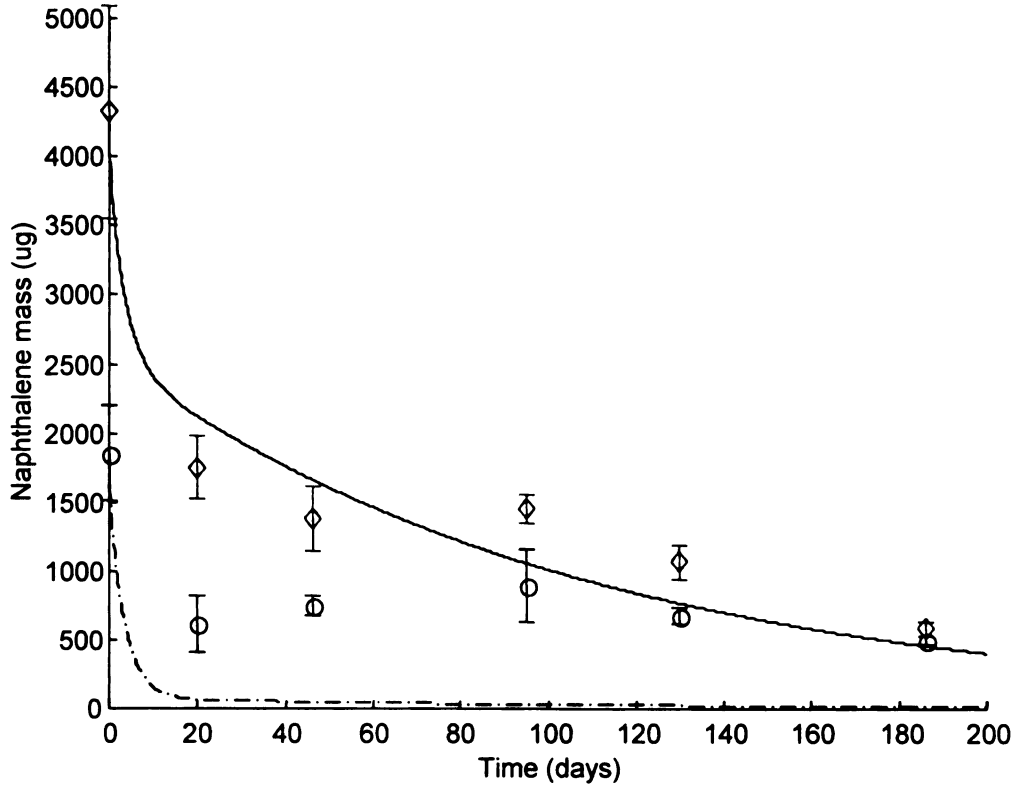

Figure 4-10. Plot of methanol extractable naphthalene mass and water extractable naphthalene mass versus time for Kal A soil that is unplanted. The diamonds (◊) are the methanol extraction data and the circles (○) are the water extraction data. Standard deviation error bars are included on each point. The solid line is the model fit of the methanol extraction data and the dashed line is the model fit of the water extraction data.

Table 4-1. Soil parameters for Spinks A and Kalkaska A soils

Soil type	n	θ_w	ρ_b	K_d	K_H	D_g
SpAf	0.5	0.15	1.25	5.0	$1.74 \cdot 10^{-2}$	22.4
Kal A	0.5	0.15	1.54	13.64	$1.74 \cdot 10^{-2}$	185

Table 4-2. Estimated parameters for planted and unplanted soils.

Soil type	Unplanted f_{eq}^{m}	Unplanted f_{neq}^{m}	Unplanted k_{neq}^{m} (hr^{-1})	*A. gerardii* k_p (hr^{-1})	*M. alba* k_p (hr^{-1})
SpAf	0.357±0.009	0.583±0.009	0.0010±0.0003	0.142±0.010	0.156±0.011
Kal A	0.272±0.004	0.564±0.008	0.0013±0.0002	0.072±0.024	0.056±0.022

References

1. Mougin, C., *Bioremediation and phytoremediation of industrial PAH-polluted soils.* Polycyclic Aromatic Compounds, 2002. **22**: p. 1011-1043.

2. Schnoor, J.L., et al., *Phytoremediation of organic and nutrient contaminants.* Environmental Science and Technology, 1995. **29**(7): p. 318A-323A.

3. Reilley, K.A., M.K. Banks, and A.P. Schwab, *Dissipation of polycyclic aromatic hydrocarbons in the rhizosphere.* Journal of Environmental Quality, 1996. **25**: p. 212-219.

4. Burken, J.G. and J.L. Schnoor, *Phytoremediation: plant uptake of atrazine and role of root exudates.* Journal of Environmental Engineering, 1996. **122**(11): p. 958-963.

5. McCutcheon, S.C. and J.L. Schnoor, *Overview of phytotransformation and control of wastes*, in *Phytoremediation: Transformation and Control of Contaminants*, S.C. McCutcheon and J.L. Schnoor, Editors. 2003, John Wiley and Sons, Inc.: Hoboken, New Jersey. p. 3-58.

6. Cunningham, S.D. and W.R. Berti, *Remediation of contaminated soils with green plants: an overview.* In Vitro Cellular and Developmental Biology, 1993. **29**: p. 207-212.

7. Cunningham, S.D., W.R. Berti, and J.W. Huang, *Phytoremediation of contaminated soils.* Trends in Biotechnology, 1995. **13**: p. 393-397.

8. Davis, L.C., et al., *Modeling the effects of plants on the bioremediation of contaminated soil and ground water.* Environmetanl Progress, 1993. **12**(1): p. 67-75.

9. Siciliano, S.D. and J.J. Germida, *Mechanisms of phytoremediation: biochemical and ecological interactions between plants and bacteria.* Environmental Reviews, 1998. **6**: p. 65-79.

10. Shimp, J.F., et al., *Beneficial effects of plants in the remediation of soil and groundwater contaminanted with organic materials.* Critical Reviews of Environmental Science and Technology, 1993. **23**(1): p. 41-77.

11. Alexander, M., *Aging, bioavailability, and overestimation of risk from environmental pollutants.* Environmental Science and Technology, 2000. **34**(20): p. 4259-4265.

12. Bosma, T.N.P., et al., *Mass transfer limitation of biotransformation: quantifying bioavailability.* Environmental Science and Technology, 1997. **31**(1): p. 248-252.

13. Chung, N. and M. Alexander, *Differences in sequestration and bioavailability of organic compounds aged in dissimilar soils.* Environmental Science and Technology, 1998. **32**(7): p. 855-860.

14. Cuypers, C., et al., *The estimation of PAH bioavailability in contaminated sediments using hydroxypropyl -B-cyclodextrin and Triton X-100 extration techniques.* Chemosphere, 2002. **46**: p. 1235-1245.

15. Feng, Y., et al., *Bioavailability of soil-sorbed biphenyl to bacteria.* Environmental Science Technology, 2000. **34**: p. 1977-1984.

16. Park, J.-H., *Bioavailability of sorbed organic contaminants*, in *Department of Civil and Environmental Engineering*. 2000, Michigan State University.

17. Zhang, W., E. Bouwer, and W. Ball, *Bioavailability of hydrophobic organic contaminants: effects and implications if sorption-related mass transfer on bioremediation.* Ground Water Monitoring and Remediation, 1998: p. 126-138.

18. Aprill, W. and R.C. Sims, *Evaluation of the use of prairie grasses for stimulating polycyclic aromatic hydrocarbon treatment in soil.* Chemosphere, 1990. **20**(1-2): p. 253-265.

19. Qui, X., et al., *Grass-enhanced bioremediation for clay soils contaminated with polynuclear aromatic hydrocarbons*, in *Bioremediation Through Rhizosphere Technology*, T.A. Anderson and J.R. Coates, Editors. 1994, American Chemical Society: Washington, D.C. p. 142-157.

20. Pradhan, S.P., et al., *Potential of phytoremediation for treatment of PAHs in soil at MGP sites.* Journal of Soil Contaminantion, 1998. **7**: p. 467-480.

21. Banks, M.K., E. Lee, and A.P. Schwab, *Evaluation of dissipation mechanisms for benzo a pyrene in the rhizosphere of tall fescue.* Journal of Environmental Quality, 1999. **28**(1): p. 294-298.

22. Chen, Y., M. Banks, and A. Schwab, *Pyrene degradation in the rhizosphere of tall fescue (Festuca arundinacea) and switchgrass (Panicum virgatum L.).* Environmental Science & Technology, 2003. **37**: p. 5778-5782.

23. Liste, H.-H. and M. Alexander, *Accumulation of phenanthrene and pyrene in rhizosphere soil.* Chemosphere, 2000. **40**: p. 11-14.

24. Muratova, A., et al., *Plant-rhizosphere-microflora association during phytoremediation of PAH-contaminated soil.* International Journal of Phytoremediation, 2003. **5**(2): p. 137-151.

25. Schwab, A.P. and M.K. Banks, *Biologically mediated dissipation of polyaromatic hydrocarbons in the root zone*, in *Bioremediation Through Rhizosphere Technology*, T.A. Anderson and J.R. Coates, Editors. 1994, American Chemical Society: Washington, D.C. p. 132-141.

26. White, J.C. and M. Alexander, *Reduced biodegradability of desorption-resistant fractions of polycyclic aromatic hydrocarbons in soil and aquifer solids.* Environmental Toxicology and Chemistry, 1996. **15**(11): p. 1973-1978.

27. Guerin, W.F. and S.A. Boyd, *Bioavailability of naphthalene associated with natural and synthetic sorbents.* Water Resources, 1997. **31**(6): p. 1504-1512.

28. Park, J.-H., X. Zhao, and T.C. Voice, *Development of a kinetic basis for bioavailability of sorbed naphthalene in soil slurries.* Water Research, 2002. **36**: p. 1620-1628.

29. Park, J.-H., X. Zhao, and T.C. Voice, *Biodegradation of non-desorbable naphthalene in soils.* Environmental Science and Technology, 2001. **35**(13): p. 2734-2740.

30. Park, J.-H., et al., *Assessment of bioavailability of soil-sorbed atrazine.* Applied and Environmental Microbiology, 2003. **69**(6): p. 3288-3298.

31. Olson, P.E., K.F. Reardon, and E.A.H. Pilon-Smits, *Ecology of rhizosphere bioremediation*, in *Phytoremediation: Transformation and Control of Contaminants*, S.C. McCutcheon and J.L. Schnoor, Editors. 2003, John Wiley and Sons, Inc.: Hoboken, New Jersey. p. 317-353.

32. Park, K.S., et al., *Fate of PAH compounds in two soil types: influence of volatilization, abiotic loss and biological activity.* Environmental Toxicology and Chemistry, 1990. **9**: p. 187-195.

33. Hickey, W.J. and J. Paek, *Ventilation effects on mineralization and volatilization of naphthalene in a gasoline-contaminanted subsurface soil.* Chemosphere, 1996. **32**(8): p. 1655-1667.

34. Ahn, I.-S., L.W. Lion, and M.L. Shuler, *Microscale-based modeling of polynuclear aromatic hydrocarbon transport and biodegradation in soil.* Biotechnology and Bioengineering, 1996. **51**: p. 1-14.

35. Gunther, T., U. Dornberger, and W. Fritsche, *Effects of ryegrass on biodegradation of hydrocarbons in soil.* Chemosphere, 1996. **33**(2): p. 203-215.

36. Heitkamp, M.A., J.P. Freeman, and C.E. Cerniglia, *Naphthalene biodegradation in environmental microcosms: estimates of degradation rates and characterization of metabolites.* Applied and Environmental Microbiology, 1987. **53**(1): p. 126-136.

37. Yolcubal, I., et al., *Biodegradation during contaminant transport inporous media: v. teh influence of growth and cell elution of microbial distribution.* Journal of Environmental Quality, 2002. **31**: p. 1824-1830.

38. Hatzinger, P. and M. Alexander, *Effect of aging of chemicals in soil on their biodegadability and extractability.* Environmental Science and Technology, 1995. **29**(2): p. 537-545.

39. Kilbane II, J., *Extractability and subsequent biodegradation of PAHs from contaminated soil.* Water, Air, and Soil Pollution, 1998. **104**: p. 285-304.

40. Northcott, G.L. and K.C. Jones, *Partitioning, extractability, and formation of nonextractable PAH residues in soil. 1. Compound differences in aging and sequestration.* Environmental Science and Technology, 2001. **35**(6): p. 1103-1110.

41. Northcott, G.L. and K.C. Jones, *Partitioning, extractability, and formation of nonextractable PAH residues in soil. 2. Effects on compound dissolution behavior.* Environmental Science and Technology, 2001. **35**(6): p. 1111-1117.

42. Millington, R. and J. Quirk, *Permeability of porous solids.* Transactions of the Faraday Society, 1961. **57**: p. 1200-1207.

43. Hallmann, J., et al., *Bacterial endophytes in agriculutural crops.* Canadian Journal of Microbiology, 1997. **43**: p. 895-914.

44. Lamb, T.G., D.W. Tonkyn, and D.A. Kluepfel, *Movement of Pseudomonas aureofaciens from the rhizosphere to aerial plant tissue.* Canadian Journal of Microbiology, 1996. **42**: p. 1112-1120.

45. Bell, C.R., et al., *Endophytic bacteria in grapevine.* Canadian Journal of Microbiology, 1995. **41**: p. 46-53.

46. Zinniel, D.K., et al., *Isolation and characterization of endophytic colonizing bacteria from agronomic crops and prairie plants.* Applied and Environmental Microbiology, 2002. **68**(5): p. 2198-2208.

47. Macleod, C. and K. Semple, *Sequential extraction of low concetrations of pyrene and formation of non-extractable residues in sterile and non-sterile soils.* Soil Biology & Biochemistry, 2003. **35**: p. 1443-1450.

48. Park, J.-H., X. Zhao, and T. Voice, *Biodegradation of non-desorbable naphthalene in soils.* Environmental Science and Technology, 2001. **35**(13): p. 2734-2740.

49. Lindhardt, B. and T.H. Christensen, *Measured and estimated volatilisation of naphthalene from a sandy soil.* Chemosphere, 1994. **29**(7): p. 1407-1419.

50. Brusseau, M.L., R.E. Jessup, and P.S.C. Rao, *Modeling the transport of solutes influenced by multiprocess nonequilibrium.* Water Resources Research, 1989. **25**(9): p. 1971-1988.

51. Brusseau, M.L., R.E. Jessup, and P.S.C. Rao, *Nonequilibrium sorption of organic chemicals: elucidation of rate-limiting processes.* Environmental Science and Technology, 1991. **25**(1): p. 134-142.

52. Brusseau, M.L. and P.S.C. Rao, *Influence of sorbate structure on nonequilibrium sorption of organic compounds.* Environmental Science and Technology, 1991. **25**(8): p. 1501-1506.

53. Hwang, S. and T. Cutright, *Evidence of underestimation in PAH sorption/desorption due to system nonequilibrium and interaction with soil constituents.* Journal of environmental Science and Health, 2004. **39**: p. 1147-1162.

54. Rahman, M., F. Amiri, and E. Worch, *Application of the mass transfer model for describing nonequilibrium transport of HOCs through natural geosorbents.* Water Research, 2003. **37**: p. 4673-4684.

55. Rao, P.S.C., J.M. Davidson, and H.M. Selim, *Evaluation of conceptual models for describing nonequilibrium adsorption-desorption of pesticides during steady-flow in soils.* Soil Science Society of Americal Journal, 1979. **43**: p. 22-28.

56. Park, J.-H., X. Zhao, and T.C. Voice, *Comparison of biodegradation kinetic parameters for naphthalene in batch and sand column systems by Pseudomonas putida.* Environmental Progress, 2001. **20**(2): p. 93-102.

57. Cornelissen, G., P.C.M. van Noort, and H.A.J. Govers, *Mechanism of slow desorption of organic compounds from sediments: A study using model sorbents.* Environmental Science and Technology, 1998. **32**: p. 3125-3131.

58. Cornelissen, G., et al., *Temperature dependence of slow adsorption and desorption kinetics of organic compounds in sediments.* Environmental Science and Technology, 1997. **31**: p. 454-460.

59. Farrell, J., D. Grassian, and M. Jones, *Investigation of mechanisms contributing to slow desorption of hydrophobic organic compounds from mineral solids.* Environmental Science and Technology, 1999. **33**: p. 1237-1243.

60. Reeves, W., et al., *Partitioning ans desorption behavior of polycyclic aromatic hydocarcon from disparate aources.* Science of the Total Environment, 2004.

61. Sharer, M., et al., *Aging effects on the sorption-desorption characteristics of anthropogenic organic compounds in soil.* Journal of Environmental Quality, 2003. **32**: p. 1385-1392.

62. Steinberg, S., J.J. Pignatello, and B. Sawhney, *Persistence of 1,2-Dibromoethane in soils: entrapment in intraparticle micropores.* Environmental Science and Technology, 1997. **31**: p. 1201-1208.

63. Li, J. and C.J. Werth, *Slow desorption mechanisms of volatile organic chemical mixtures in soil and sediment micropores.* Environmental Science and Technology, 2004. **38**: p. 440-448.

64. Briggs, G.G., R.H. Bromilow, and A.A. Evans, *Relationships between lipophilicity and root uptake and translocation of non-ionised chemicals in barley.* Pesticide Science, 1982. **13**: p. 495-504.

65. Emerman, S.H. and T.E. Dawson, *Experiments using split-root chambers on water uptake from soil macropores by sunflowers.* Plant and Soil, 1997. **189**: p. 57-63.

Chapter 5. Using an effectiveness factor to improve decision making regarding phytoremediation

Abstract

The development of an effectiveness factor for improving decision making in phytoremediation is addressed. This effectiveness factor compares the remediation rates in planted and unplanted systems. A plot of the effectiveness factor versus the Thiele modulus (i.e. a dimensionless ratio of reactive processes to mass transfer processes) was divided into three regimes. These regimes reveal the efficacy of phytoremediation and the mechanisms that limit the rate of remediation in planted systems. At low values of the Thiele modulus, phytoremediation does not significantly enhance the remediation rate. At moderate values, phytoremediation improves the remediation rate, but is limited by the kinetics of plant uptake or plant facilitated degradation. At large values of the Thiele modulus, the use of plants remains beneficial, though improving the remediation rate relies on enhancing the contaminant desorption rate. Systems that are completely desorption limited benefit less from being planted, as desorption is regarded as a necessary first step in a contaminant's remediation. To overcome this limitation, further exploration is needed regarding plant species that are capable of enhancing the contaminant desorption rate or enhancing contaminant bioavailability. Desorption limitations impact the decision making process by directing the site engineer to technologies that are capable of overcoming these limitations.

Introduction

This chapter presents a method to determine whether phytoremediation provides enhanced contaminant removal when compared to other remediation strategies. The result of this comparison is improved decision making regarding the use of plants to enhance contaminant removal. Increased use of phytoremediation in the field has made the pursuit of improved decision making important. The decision to use phytoremediation depends upon the cost, extent, and rate of removal using plants versus the cost, extent, and rate of removal using other technologies. Cost, extent, and rate of removal are at least partially dependent upon the physicochemical properties of the contaminant and soil, and the biological properties of the selected technology (i.e. phytoremediation, bioaugmentation, natural attenuation, etc.). These properties are measured, either *in vitro* or *in situ*, and used to formulate mechanisms, either descriptive (empirical) or explanatory (theoretical), that can be used to construct mathematical models. These mathematical models are typically used in a predictive mode after the accuracy and uncertainty of the models have been assessed by comparing experimental data with model simulations. Once the robustness of a model has been accepted, a method is needed for interpreting the model output to make decisions regarding the use of a clean-up technology (e.g. phytoremediation). The method presented here is borrowed from the discipline of heterogeneous catalysis. In heterogeneous catalysis—particularly catalysis involving diffusion and reaction inside catalyst particles—chemical reactants diffuse through the catalyst pore structure, adsorb to the catalyst surface, react, and the resulting products desorb and subsequently diffuse through the pore structure and into the surrounding fluid. Briefly, the mathematical model that describes/explains this process is

appropriately nondimensionalized to form a dimensionless group named the Thiele modulus. A "rating factor", or effectiveness factor, is defined to compare the rate of reaction with pore diffusion resistance to the rate of reaction at the surface conditions[1]. By plotting the effectiveness factor versus the Thiele modulus, a profile is generated that can be divided into two regimes: 1) a reaction rate limited regime at low values of the Thiele modulus, and 2) a mass transfer limited regime at high values of the Thiele modulus. Improving the overall reaction rate by catalyst selection is predicated on which regime characterizes the catalyzed reaction. By analogy, decision making in phytoremediation can benefit from the same strategy used in heterogeneous catalysis. What is needed is the selection of a suitable effectiveness factor, the division of limiting behavior into discrete regimes, and a means of determining the regime in which a given phytoremediation systems resides. The use or nonuse of phytoremediation can then be determined. The aim of this paper is to use this methodology to improve decision making regarding phytoremediation.

The mechanisms thought to be important for phytoremediation of PAHs include plant uptake, sorption to roots, and degradation by rhizosphere microbes (depicted in Figure 5-1). Plant uptake[2, 3] is more important for the lower molecular weight PAHs, as these tend to be more soluble and less hydrophobic. The amount of contaminant sorbed to roots depends on the relative hydrophobicities of the root lipid fraction and the contaminant[4]. The promotion of degrading organisms in the rhizosphere by root exudation or secretion is called phytostimulation. Phytostimulation[5, 6] is a proposed mechanism for the enhanced remediation of PAHs—especially the higher molecular weight PAHs.

As several mechanisms are responsible for a plant's ability to remove or affect the removal of contaminants, several limiting phenomena may ultimately be responsible for slowing cleanup. Greatest among these is the contaminant's desorption from the soil matrix. The processes responsible for increased degradation by plants act after the contaminant is thought to have desorbed. For example, microbial biodegradation has been demonstrated to occur after the contaminant desorbs. Also, plant uptake of organic contaminants occurs after the contaminant desorbs from the soil matrix. Volatilization and leaching of the contaminant are also dependent upon prior desorption. Determining the rate and extent of the mass transfer limitations is a necessary first step before applying phytoremediation. If the contaminant is not limited by desorption, then comparing the rates of the various processes remains an important matter. This comparison may lead to the best method for enhancing the rate, whether degradation can be enhanced by nutrient amendment, or whether a plant species that transpires more water can be selected to hasten uptake. The formulation of a suitable effectiveness factor would encompass the mechanisms present in planted and unplanted systems. Classical plots of the effectiveness factor can be used to compare the rates of removal in planted and unplanted treatments. Furthermore, these plots can be divided into regimes that correspond to the various removal controlling mechanisms. Decision making is guided by determining the regime a given planted system resides.

Mathematics

The model presented in Equations 5-1 through 5-3 was used to describe the unplanted scenario for this investigation. A list of model variables and model parameters is presented in Table 5-1. This model was formulated to describe the transport and reactions of naphthalene in the Spinks A-horizon soil.

$$\theta_w \frac{\partial C_w}{\partial t} + \rho_b \frac{\partial S_{eq}}{\partial t} + \rho_b \frac{\partial S_{neq}}{\partial t} + \rho_b \frac{\partial S_{im}}{\partial t} + \theta_g \frac{\partial C_g}{\partial t} = D_{g,e}\theta_g \frac{\partial^2 C_g}{\partial z^2} \qquad \text{Equation (5-1)}$$

$$\frac{\partial S_{neq}}{\partial t} = -k_{neq}\left(S_{neq} - K_d f_{neq} C_w\right) \qquad \text{Equation (5-2)}$$

$$\frac{\partial S_{im}}{\partial t} = 0 \qquad \text{Equation (5-3)}$$

A second model, presented as Equations 5-4 through 5-6, was formulated to describe the action of the plant in a first-order kinetic manner.

$$\theta_w \frac{\partial C_w}{\partial t} + \rho_b \frac{\partial S_{eq}}{\partial t} + \rho_b \frac{\partial S_{neq}}{\partial t} + \rho_b \frac{\partial S_{im}}{\partial t} + \theta_g \frac{\partial C_g}{\partial t} = D_{g,e}\theta_g \frac{\partial^2 C_g}{\partial z^2} - k_p \theta_w C_w \qquad \text{Equation (5-4)}$$

$$\frac{\partial S_{neq}}{\partial t} = -k_{neq}\left(S_{neq} - K_d f_{neq} C_w\right) \qquad \text{Equation (5-5)}$$

$$\frac{\partial S_{im}}{\partial t} = -\frac{k_p \theta_w}{\rho_b K_d + \theta_w} S_{im} \qquad \text{Equation (5-6)}$$

Both models divide the soil into three domains. The equilibrium domain is parameterized by the soil-water partition coefficient, assuming that transfer from the soil to the water

occurs instantaneously. The first-order desorption rate coefficient parameterizes the rate of transport from the mass transfer limited domain (a.k.a. the nonequilibrium domain) of the soil. The models consider the volatilization of naphthalene to occur by Henry's partitioning into the soil gas, followed by gaseous diffusion out of the system boundary. An immobile soil domain is constructed to represent material that does not volatilize. The phytoremediation model, presented in Equations 5-4 through 5-6, considers that the remediation of naphthalene is described by first-order kinetics. This description includes phytoremediation in the immobile soil solution and the solution that is in equilibrium with the soil gas. A box model depicting the transport and reactive processes included in both models is presented in Figure 5-2.

The nondimensionalization of the unplanted model results in Equations 5-7 through 5-9.

$$R_1 \frac{\partial C_w^*}{\partial \tau} + R_2 \frac{\partial S_{neq}^*}{\partial \tau} + R_3 \frac{\partial S_{im}^*}{\partial \tau} = R_4 Da \frac{\partial^2 C_w^*}{\partial Z^2} \qquad \text{Equation (5-7)}$$

$$\frac{\partial S_{neq}^*}{\partial \tau} = -\left(S_{neq}^* - C_w^*\right) \qquad \text{Equation (5-8)}$$

$$\frac{\partial S_{im}^*}{\partial \tau} = 0 \qquad \text{Equation (5-9)}$$

Likewise, the nondimensionalization of the phytoremediation model gives Equations 5-10 through 5-12.

$$R_1 \frac{\partial C_w^*}{\partial \tau} + R_2 \frac{\partial S_{neq}^*}{\partial \tau} + R_3 \frac{\partial S_{eq.mic}^*}{\partial \tau} = R_4 Da \frac{\partial^2 C_w^*}{\partial Z^2} - \phi^2 C_w^* \qquad \text{Equation (5-10)}$$

$$\frac{\partial S^{\bullet}_{neq}}{\partial \tau} = -\left(S^{\bullet}_{neq} - C^{\bullet}_{w}\right)$$ Equation (5-11)

$$\frac{\partial S^{\bullet}_{im}}{\partial \tau} = -R_5 S^{\bullet}_{im}$$ Equation (5-12)

A list of dimensionless model variables and parameters is presented in Table 5-2. Comparisons between planted and unplanted remediation were made using an effectiveness factor. Historically, the effectiveness factor approach was used to describe heterogeneous catalysis. This construct is defined as the ratio of the rate of reaction that includes a diffusive resistance to the rate of reaction at the solid catalyst surface. An effectiveness factor equal to one corresponds to a system that is limited by the reaction rate. An effectiveness factor that is lower than one corresponds to a system that is limited by mass transfer inside the catalyst pellet. Determining whether mass transfer or reaction is limiting the rate of product formation defines how reaction can be increased. By analogy, this effectiveness factor approach can be used to compare the rate of contaminant remediation between planted and unplanted systems. The rate of contaminant removal is compared by selecting an arbitrary growing season of 200 days. Mathematically, this effectiveness factor is presented in Equation 5-13.

$$\eta = \frac{\left(\left(\text{mass of contaminant at t} = 0\right) - \left(\text{mass of contaminant at t} = 200\right)\right)_{\text{planted}}}{\left(\left(\text{mass of contaminant at t} = 0\right) - \left(\text{mass of contaminant at t} = 200\right)\right)_{\text{unplanted}}}$$

Equation (5-13)

The effectiveness factor is typically plotted against a dimensionless number called the Thiele modulus. In the field of heterogeneous catalysis, this modulus is the ratio of reaction processes to mass transfer processes. The reaction processes are typically parameterized by reaction rate coefficients and the mass transfer processes are typically parameterized by diffusivities. The Thiele modulus, presented in Equation 5-14, is formulated in an analogous manner for this study.

$$\phi = \sqrt{\frac{k_p}{k_{neq}}} \qquad \text{Equation (5-14)}$$

In this description, the kinetic forces are parameterized by k_p, which encompasses the combined effect of transpirational uptake and phytostimulation. The mass transfer forces are parameterized by k_{neq}, which parameterizes the rate of contaminant desorption from the soil matrix. Plots of the effectiveness factor versus the Thiele modulus can be divided into discrete regimes of behavior. An interpretation of these regimes reveals whether phytoremediation is an effective technology when compared to remediation in an unplanted system.

Results and Discussion

Figure 5-3 contains a plot of the effectiveness factor versus the Thiele modulus using a parameter set determined for naphthalene which is presented in Table 5-3. At small values of the Thiele modulus, the effectiveness factor approaches a value of one. In this situation, the magnitude of the plant's effect on remediation is small, thus an unplanted treatment remediates the system as well as the planted treatment. At intermediate values of the Thiele modulus, the slope of the curve becomes positive. The planted system enhances remediation in this transition regime. At relatively large values of the Thiele modulus, the curve begins to approach a zero slope. This situation arises when contaminant mass transfer is slow compared to the potential remediation rate of the planted system. At large values of the Thiele modulus, there is no benefit in increasing the transpirational flow, because slow mass transfer eventually limits remediation. The slope of the curve approaches zero as rate-limited mass transfer controls the remediation rate in planted and unplanted systems alike. Regime-one behavior corresponds to no benefit to remediation by plants, a situation that occurs at low values of the Thiele modulus. Regime two is characterized by plant enhanced remediation, though the remediation rate is limited by some activity associated with the plant. Regime three also displays enhanced remediation, though the remediation rate has become limited by contaminant mass transfer from the soil. It is important to note that enhanced mass transfer is not included in the model formulation (i.e. enhanced remediation is defined as the increased remediation rate in planted systems when compared to unplanted systems).

Figure 5-4 is a plot showing the effect of increasing the Damkohler number on the effectiveness factor. The parameter values used to plot Figures 5-3 through 5-7 are contained in Table 5-4. Increasing the Damkohler number decreases the value of the effectiveness factor. Mechanistically, increased Damkohler numbers are the results of increasing the effective diffusivity relative to the desorption rate coefficient. Increasing the effective soil gas diffusivity increases the rate of contaminant volatilization. Systems with high volatilization rates are not likely to be improved by planting. However, soils with significant tortuosities (e.g. soils that require the Millington-Quirk correction[7]) are likely to be amenable to phytoremediation as the volatilization rate of semi-volatiles will be reduced. Furthermore, increasing the effective diffusivity does alter the shape of the profile. Specifically, the presence of the third regime suggests that rate-limited mass transfer limits contaminant volatilization. Rate-limited transfer, present in the third regime, is responsible for limiting both volatilization and phytoremediation.

Figure 5-5 is a plot showing the effect of increasing the value of K_d on the effectiveness factor. This is equivalent to selecting another contaminant with a larger octanol-water coefficient or selecting a soil with a larger amount of organic matter. Increasing K_d, results in increasing the effectiveness factor, as seen from Figure 5-5. An increased effectiveness factor corresponds to a beneficial circumstance in planted systems. Three-ring PAHs, such as phenanthrene and anthracene, are more likely to benefit from phytoremediation than a two-ring PAH. Increased hydrophobicity leads to a larger amount of contaminant in the soil matrix, particularly the soil organic matter. Thus the amount of contaminant in the soil solution is decreased, which decreases the amount in equilibrium with the soil gas. Consequently, the amount of contaminant available for

volatilization is decreased. Again, decreased volatilization leads to increased effectiveness factors. The greater the effectiveness factor, the more responsive is the system to the plant.

Figure 5-6 is a plot comparing different values of the desorption rate coefficient. The effectiveness factor for phytoremediation increases with decreasing values of the desorption rate coefficient. As the rate of mass transfer from the soil matrix eventually limits the rate of volatilization, a technology that increases the driving force for mass transfer will benefit the removal of contaminant. Planted systems are superior to unplanted systems in this respect as transpirational uptake and microbial degradation serve to increase the driving force for mass transfer.

Figure 5-7 is a plot comparing systems in which the site fractions have been altered. The topmost curve ($f_{eq} = 0$) results when the equilibrium sites are converted into nonequilibrium sites. The effectiveness of phytoremediation increases in this scenario, as volatilization becomes limited by mass transfer, and contaminant removal occurs at a slower rate in the unplanted system. Conversly, converting the nonequilibrium sites into equilibrium sites reduces the effectiveness of phytoremediation when compared to the base case. As volatilization becomes a more significant mechanism for naphthalene removal, the effectiveness of phytoremediation decreases. Finally, converting the immobile site fraction into equilibrium sites resulted in a significant decrease in the effectiveness of planted systems. Though the immobile fraction only comprises 6% of the total soil domain, removing this fraction had a profound impact on the effectiveness factor. Essentially, naphthalene that is available to plant remediative processes, but is not available for volatilization, has a significant role in the effectiveness of phytoremediation

of naphthalene in SpAf soil. Simply put, increasing the amount of naphthalene available for phytoremediation that is not mobile in unplanted soils will increase the effectiveness factor for phytoremediation. A water extractable amount of contaminant, that is not removable by the mechanisms available in the unplanted system (e.g. volatilization), will tend to favor technologies that can "mobilize" this immobile component.

Decision making

From the previous analysis, determining the regime that controls contaminant remediation is useful. Contaminant remediation limited by the first regime will require an improved approach if phytoremediation is to be beneficial. Several reasons exist for remediation controlled in the first regime. The rate of transpiration relative to the rate of volatilization may be too small. This can be ameliorated by using a different plant species with a greater transpirational flow, such as *Salix* spp. (Willow). When phytoremediation is used in the phytostimulation mode, the degrading portion of the consortia may not be effectively stimulated. This limitation can be overcome through use of plant species that exude molecules chemically resembling the contaminant. The use of *Morus rubra* (Red Mulberry)[8] is an example of the stimulation of PCB degrading bacteria by exudation of phenolic compounds. These phenolic compounds induce degradative activity or promote cometabolism. The goal of increasing transpiration or enhancing phytostimulation is to shift the control of contaminant remediation from regime one to regime two or three.

Contaminant remediation controlled in the second regime is characterized by the beneficial application of phytoremediation. Unlike the first regime, plants do enhance the remediation of contaminant in the second regime. Like the first regime, the rate that

contaminants are remediated from the soil is limited by reactive processes, not mass transfer processes. Accelerating the rate of transpiration or enhancing the mechanisms of phytostimulation would benefit the overall remediation. Proper plant selection and the optimal application of nutrient amendments are options for increasing the phytoremediation rate. The effect of either of these actions is to shift the control of contaminant remediation from regime two to regime three.

Rate-limited mass transfer is the controlling mechanism in the third regime. Like the second regime, the use of plants remains beneficial when compared to an unplanted treatment. However, the rate at which phytoremediation is occurring is limited by the rate at which contaminant mass transfer is occurring. Accelerating the rate of phytoremediation depends upon a plant's ability to enhance the desorption rate from the soil matrix. This is an area that warrants further study, as plants that enhance the rate of desorption from mass transfer limited soil regimes have yet to be identified.

Approach

The general approach developed in this work does not favor the use of a particular model. The effectiveness factor can be used to compare the rate of remediation between planted and unplanted systems, while using any descriptive model (preferably a model with a degree of experimental validation). Plotting the effectiveness factor versus the Thiele modulus will result in a profile that can be divided into separate regimes. The mechanisms that govern these regimes can be illuminated by careful analysis. Decision making regarding the proper use of phytoremediation can then be made in a more informed manner.

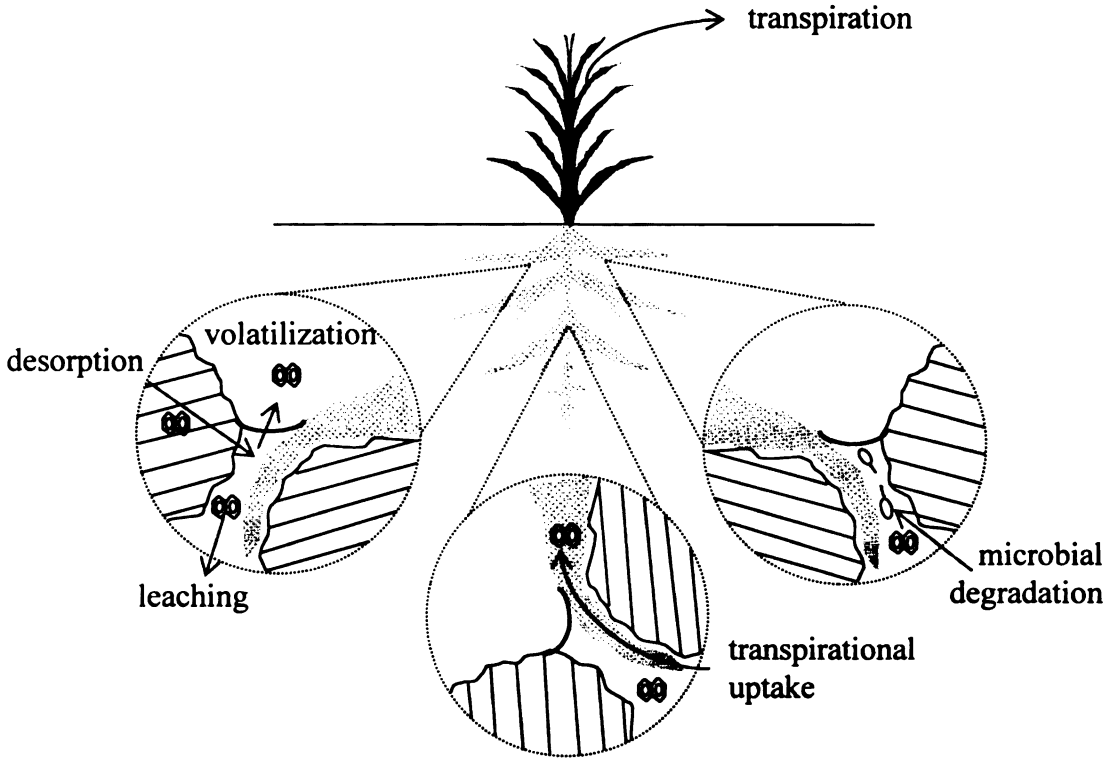

Figure 5-1. A diagram detailing some of the processes involved in the phytoremediation of naphthalene. The hatched regions represent soil aggregates.

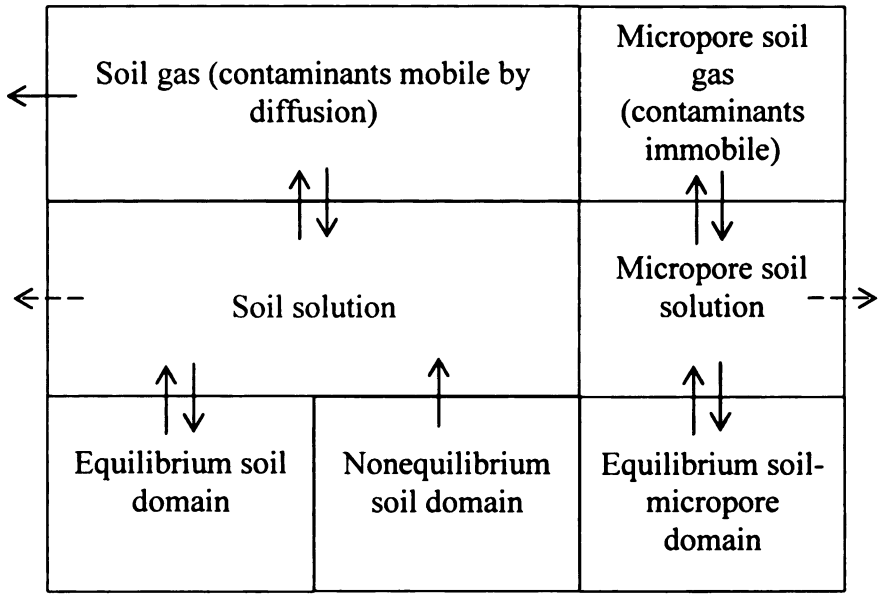

Figure 5-2. A box model of the transport and reactive processes occurring in rhizosphere soil. The double arrows represent equilibrium processes and the single arrows represent kinetic or transport processes. The dashed arrows represent the kinetic process added to the phytoremediation model.

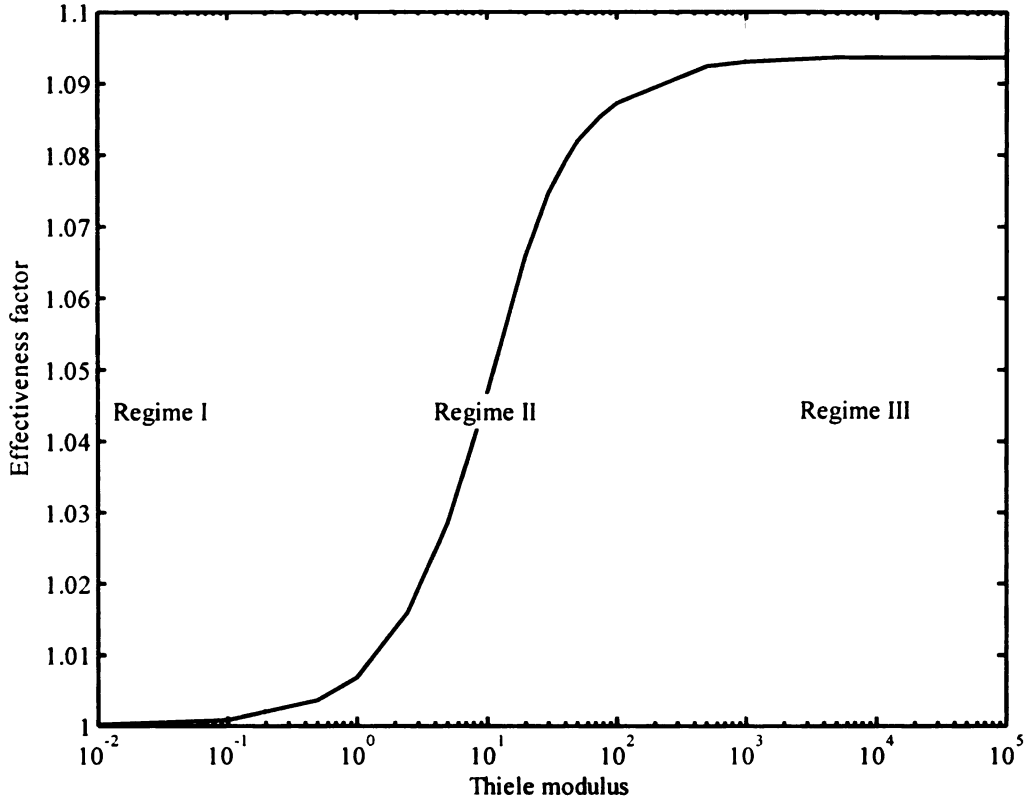

Figure 5-3. A plot demonstrating the regimes that control the phytoremediation of naphthalene in Spinks A-horizon soil.

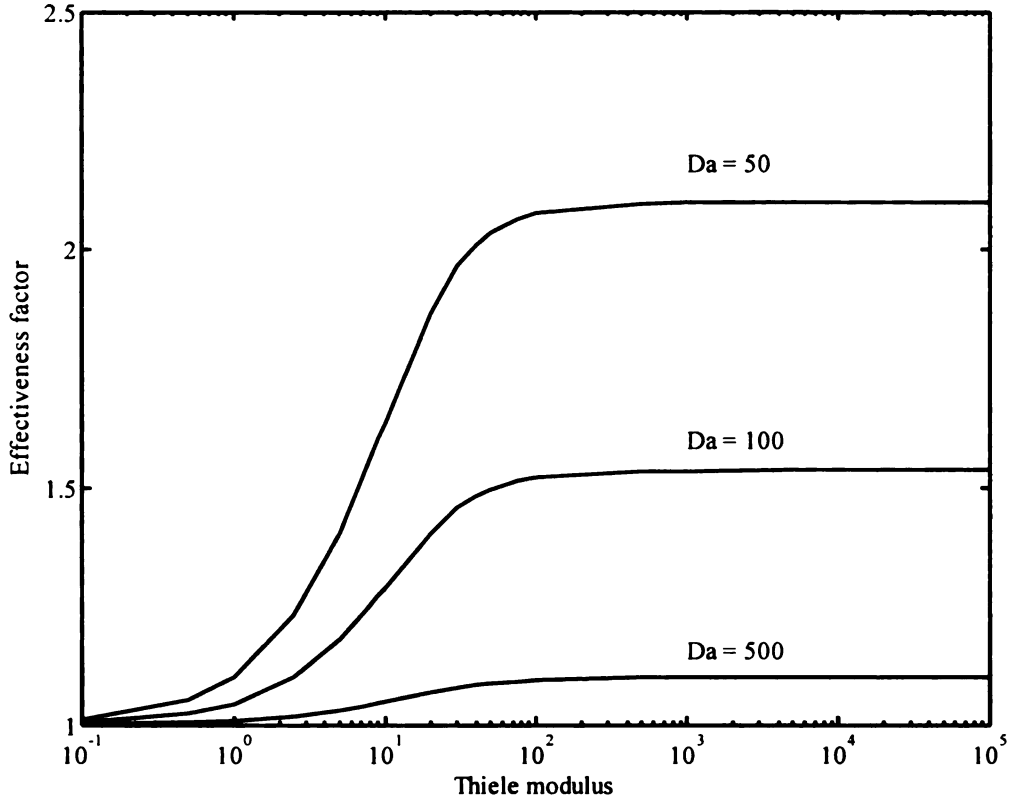

Figure 5-4. The effect of increasing the Damkohler number on the effectiveness factor.

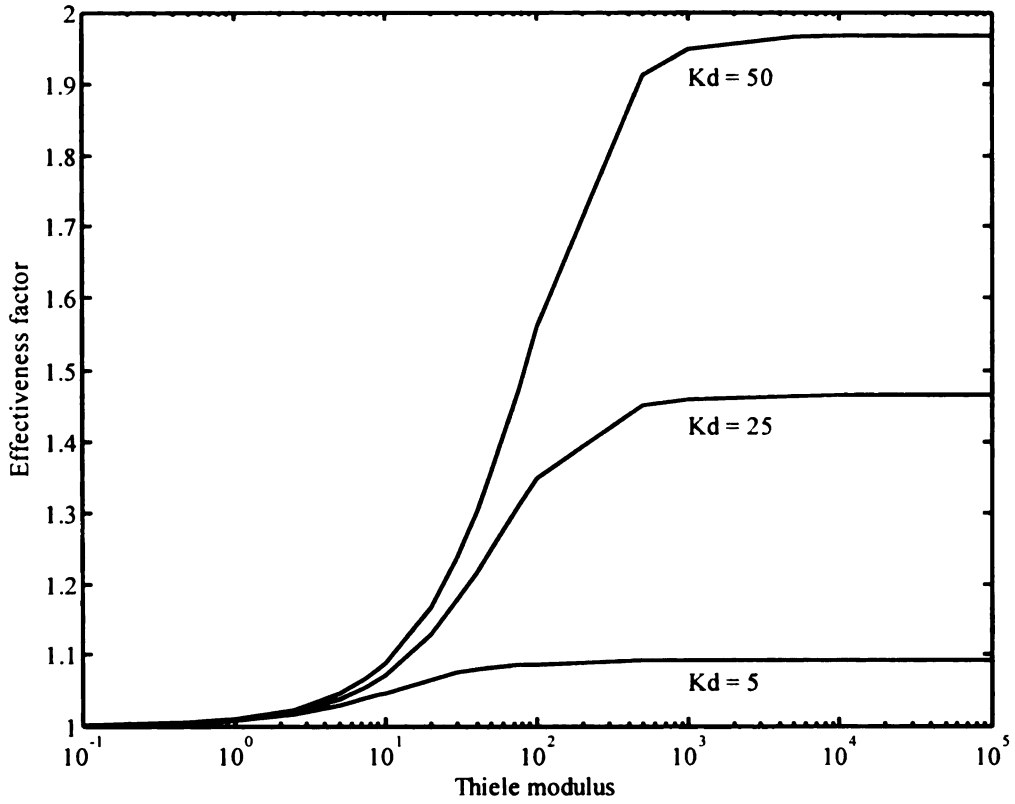

Figure 5-5. The effect of increasing the soil-water partition coefficient on the effectiveness factor.

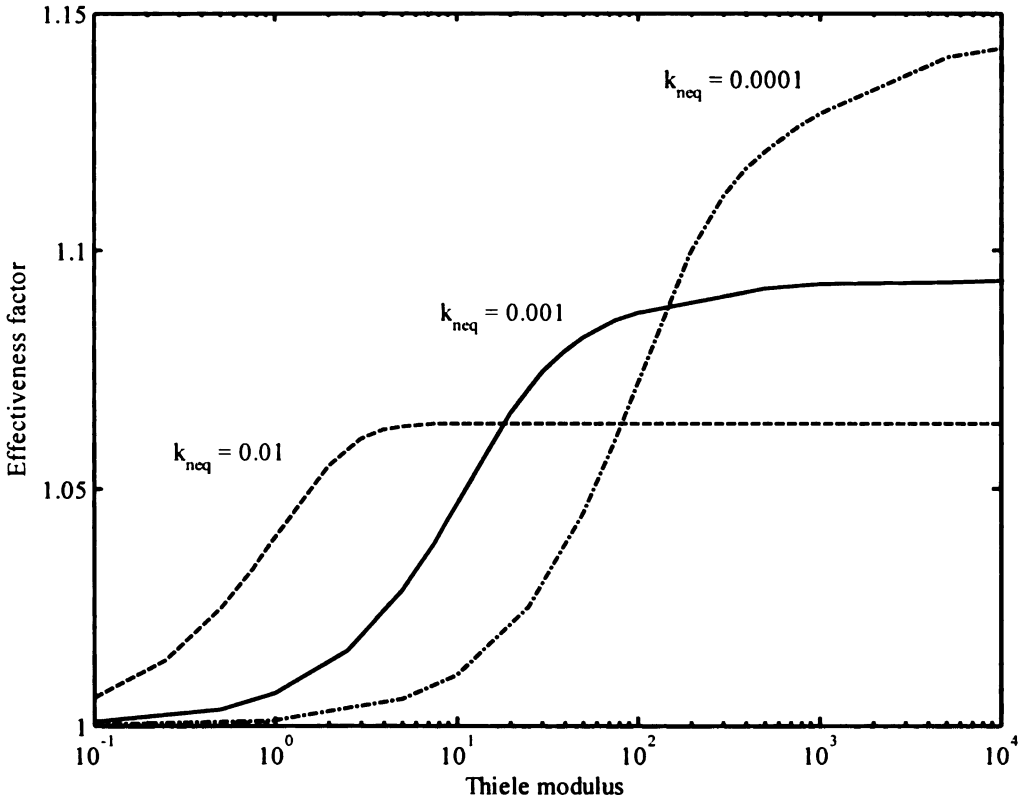

Figure 5-6. The effect of the desorption rate coefficient on the effectiveness factor.

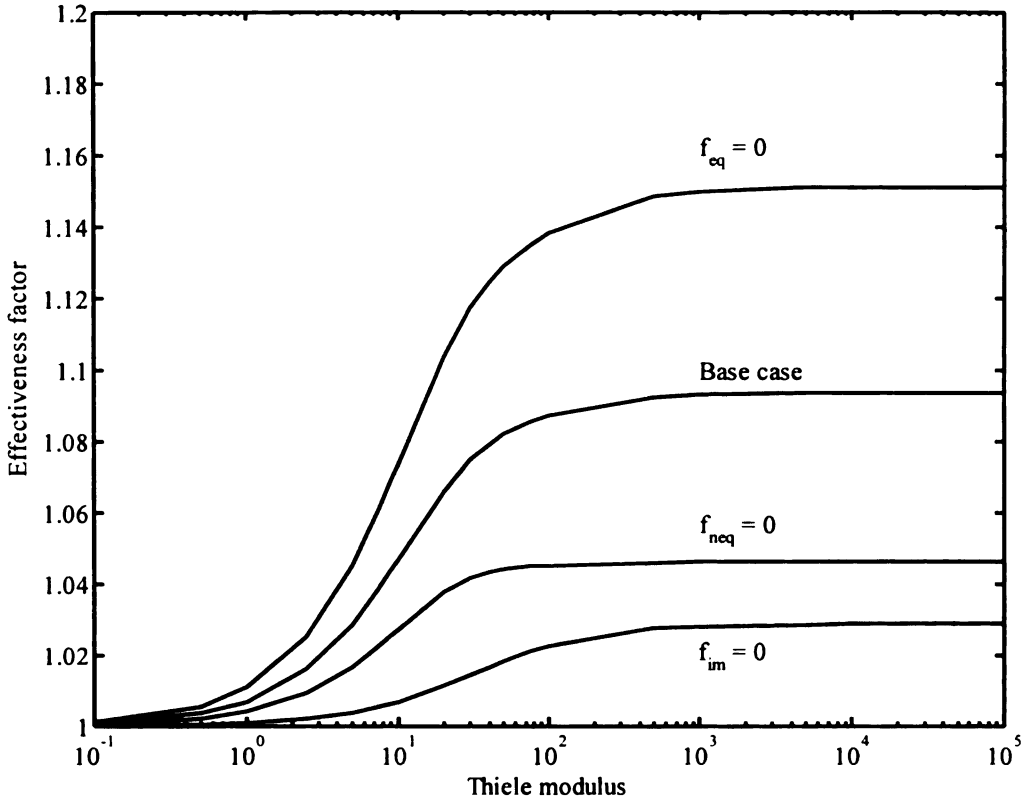

Figure 5-7. The effect of converting the equilibrium fraction to the nonequilibrium fraction ($f_{eq} = 0$), converting the nonequilibrium fraction to the equilibrium fraction ($f_{neq} = 0$), and converting the immobile fraction to the equilibrium fraction ($f_{im} = 0$).

Table 5-1. A list of model variables and parameters for the planted and unplanted mathematical models.

Variable	Description	Units
C_g	contaminant concentration in the soil gas	μg/(ml of soil gas)
C_w	contaminant concentration in the soil solution	μg/(ml of soil solution)
S_{eq}	contaminant concentration in the equilibrium-soil solid	μg/(g of soil solid)
S_{im}	contaminant concentration in the microporous equilibrium soil solid	μg/(g of soil solid)
S_{neq}	contaminant concentration in the nonequilibrium soil solid	μg/(g of soil solid)
t	time	hrs
z	vertical distance	cm
Parameter		
$D_{g,e}$	effective soil gas diffusivity	cm^2/hrs
f_{eq}	fraction of soil that is in equilibrium with the soil solution	--
f_{neq}	fraction of soil that is in nonequilibrium with the soil solution	--
f_{im}	fraction of soil that is in equilibrium with the immobile soil solution	--
K_d	soil-water partition coefficient	(ml of soil solution)/ (g of soil solid)
h	rhizosphere depth	cm
k_{neq}	first-order desorption rate coefficient	1/hrs
k_p	first-order kinetic coefficient attributed to plant action	1/hrs
θ_g	soil gas content	(ml of soil gas)/ (ml of total soil volume)
θ_w	soil moisture content	(ml of soil moisture)/ (ml of total soil volume)
ρ_b	soil bulk density	(g of dry soil)/ (ml of total soil volume)

Table 5-2. A list of dimensionless variables and parameters for the planted and unplanted mathematical models.

Dimensionless variable	Description	Structure
C_w^*	dimensionless soil solution concentration	$\frac{C_w}{C_{wo}}$ †
S_{im}^*	dimensionless microporous soil solid concentration	$\frac{S_{im}}{S_{imo}}$
S_{neq}^*	dimensionless nonequilibrium concentration	$\frac{S_{neq}}{S_{neqo}}$
η_{200}	effectiveness factor at 200 days	(amount degraded in unplanted treatments)$_{200\ days}$/ (amount degraded n planted treatments)$_{200\ days}$
τ	dimensionless time	$t \cdot k_{neq}$
Z	dimensionless vertical distance	$\frac{z}{h}$
Dimensionless groups		
Da	Damkohler number	$\frac{D_{g,e}}{k_{neq} \cdot h^2}$
R_1	Dimensionless parameter 1	$1 + \frac{\rho_b f_{eq} K_d}{\theta_w} + \frac{\theta_g H}{\theta_w}$
R_2	Dimensionless parameter 2	$\frac{\rho_b f_{neq} K_d}{\theta_w}$
R_3	Dimensionless parameter 3	$\frac{\rho_b f_{im} K_d}{\theta_w}$
R_4	Dimensionless parameter 4	$\frac{(f_{eq} + f_{neq})\theta_g H}{\theta_w}$
R_5	Dimensionless parameter 5	$\frac{\theta_w}{\rho_b K_d + \theta_w}$
ϕ	Thiele modulus	$\frac{k_p}{k_{neq}}$

† The symbol (o) denotes an initial value.

Table 5-3. Base case parameter values used for naphthalene transport and reaction in soil.

k_p	k_{neq}	f_{eq}	f_{neq}	K_d	$D_{g,e}$	H	θ_w	n
1/h	1/h	--	--	(ml soln)/ (g solid)	cm^2/h	(ml soln)/ (ml total)	(ml soln)/ (ml total)	(ml void)/ (ml total)
0.15	0.0010	0.36	0.58	5.0	22.4	0.02	0.15	0.5

Table 5-4. Dimensionless number and parameter values used to generate Figures 3 through 8.

Figure #	Da	f_{eq}	f_{neq}	f_{im}	K_d (ml soln/ g solid)	k_{neq} (1/hr)
3	552	0.36	0.58	0.06	5	0.001
4	50, 100, 500	0.36	0.58	0.06	5	0.001
5	552	0.36	0.58	0.06	5, 50, 500	0.001
6	552	0	0.94	0.06	5	0.01, 0.001, 0.0001
7 (f_{eq}=0)	552	0	0.94	0.06	5	0.001
7 (f_{neq}=0)	552	0.94	0	0.06	5	0.001
7 (f_{im}=0)	552	0.42	0.58	0	5	0.001

References

1. Froment, G.F. and K.B. Bischoff, *Chemical Reactor Analysis and Design.* 2nd ed. 1990: John Wiley and Sons, Inc.

2. Briggs, G.G., R.H. Bromilow, and A.A. Evans, *Relationships between lipophilicity and root uptake and translocation of non-ionised chemicals in barley.* Pesticide Science, 1982. **13**: p. 495-504.

3. Trapp, S. and J.C. McFarlane, eds. *Plant Contamination: Modeling and Simulation of Organic Chemical Processes.* 1 ed. 1995, Lewis Publishers: Boca Raton. 254.

4. Chiou, C.T., G. Sheng, and M. Manes, *A partition-limited model for the plant uptake of organic contaminants from soil and water.* Environmental Science and Technology, 2001. **35**: p. 1437-1444.

5. Cunningham, S.D., W.R. Berti, and J.W. Huang, *Phytoremediation of contaminated soils.* Trends in Biotechnology, 1995. **13**: p. 393-397.

6. Siciliano, S.D. and J.J. Germida, *Mechanisms of phytoremediation: biochemical and ecological interactions between plants and bacteria.* Environmental Reviews, 1998. **6**: p. 65-79.

7. Millington, R. and J. Quirk, *Permeability of porous solids.* Transactions of the Faraday Society, 1961. **57**: p. 1200-1207.

8. Leigh, M., et al., *Root turnover: an important source of microbial substrates in rhizosphere remediation of recalcitrant contaminants.* Environmental Science and Technology, 2002. **36**: p. 1579-1583.